

Figure 4. Solitary wave traveling into a reservoir

Side Channels

A series of numerical experiments was conducted to assess the influence within secondary channels of forces generated by a vessel navigating the main channel. Geometric and hydraulic parameters used to describe the features of a river side channel are shown in Figure 5. Dimensional analysis of the representative terms l , L , B , b , D , d , V , and v leads to the geometric ratios L/l , B/b , and D/d . Here, B/b and D/d describe a cross section and L/l describes the island length. Appropriate values of these descriptive ratios were determined from the Upper Mississippi River Database for Pool 8. Island lengths (L/l) vary from 3.6 to 10, so a range of island-to-vessel length ratios of 2 to 10 were modeled. Secondary channel widths (b/B) were found to vary only between 0.2 and 0.3, so the secondary-channel-to-main-channel width ratio was held constant at 0.25. Secondary channel depths (d/D) vary from 0.4 to 0.9. A range of main channel depth from 1 to 3 times the secondary channel depth was simulated.

The main channel cross section for these experiments was similar to that found at Kampsville (Plate 3). Specifically, the main channel was 306.48 m wide with a maximum depth of 4.67 m. The thalweg was located 125.54 m from the right bank. The sailing line was 1.5 m left of the thalweg.

The vessel configuration was 297.2 m long by 32.0 m wide, drafted at 2.74 m. This represented a 3-wide by 5-long barge train. The tow traveled at 2.9 m/sec.

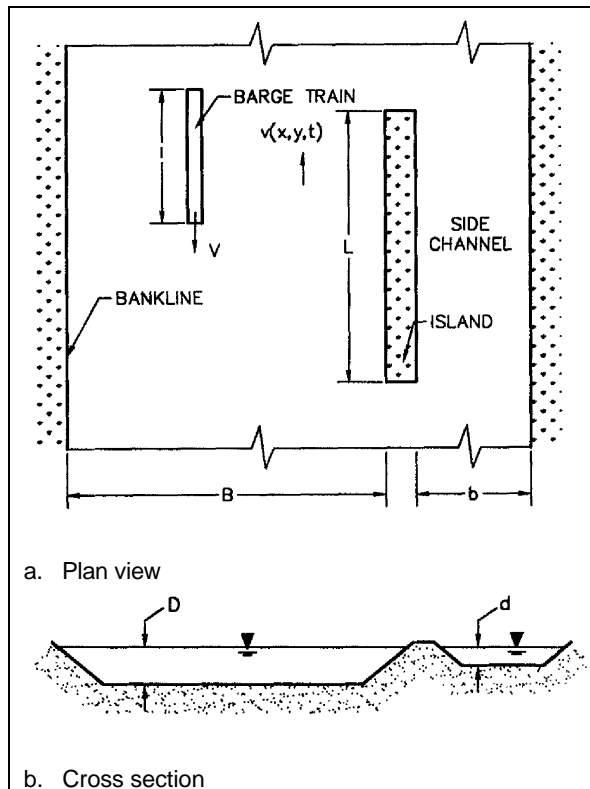


Figure 5. Geometric and hydraulic parameters describing side channels

Ambient conditions for each test were still water since vessel effects on the flow field are the interest in this study. The model parameters used for these experiments are provided in the following tabulation. Each simulation accelerated the vessel from rest to terminal speed (2.9 m/sec) in about 10.3 sec.

Schematics of the various geometries modeled and the corresponding time-histories of drawdown and current changes in the main channel and at the inlet, middle, and outlet of the secondary channel are shown in Plates 30-109. The zero abscissa is the time at which the bow of the vessel reaches the x -coordinate of the node plotted. The x -component of velocity is positive in the direction of the travel of the boat. The y velocity component is positive if it is directed into the side channel. At the entrance, the y velocity components are indicators of flow into the side channels.

Model Parameter	Value
$g, \text{ m/sec}^2$	9.81
n	0.025
C	0.1
$A, \text{ m/sec}^2$	0.2828
$T_s, \text{ sec}$	10.2552
β	0.25
α	1.5
$\Delta t, \text{ sec}$	5.128

The x-component is simply the return currents produced by the vessel. This discussion will focus on flow in the side channel rather than the return currents.

Side channels behave somewhat differently from backwaters. The depression caused by the vessel will depress the water surface at the side channel entrance initially, but thereafter, the entrance behaves like a reservoir, i.e., the water surface remains fixed. In fact, both ends of the side channel are reservoirs. So the initial depression pulse will travel to the opposite end of the side channel where it will be negatively reflected and return as a positive wave. When this positive wave reaches the original end, it will be negatively reflected again and return as a depression. A complete cycle has a period of approximately $2L/(gH)^{1/2}$. Note that at all times the velocity pulse is directed toward the entrance where the vessel originally passed. Velocities at the ends of the side channels are amplified and so are typically larger than the velocities within the side channels. The vessel will continue to move along the river, passing the other inlet of the side channel. The velocity pulse produced at this inlet will tend to cancel those generated when the vessel passed the first inlet to the side channel. So in many of these examples one will see a fairly regular velocity-wave pattern until the vessel has time to reach the opposite channel end. At this point the velocity wave magnitude will reduce and appear to have shorter wave periods.

Backwaters

Backwater parameters are displayed in Figure 6. The backwater plan shape was represented as a straight channel. Dimensionless parameters include the width of the channel into the backwater area (b/B), the measure of the backwater area length (L/l), and the measure of the backwater area depth (d/D). Two backwater-to-vessel length ratios ($L/l = 1$ and 10) were examined. Two different backwater entrance widths were simulated. The main-channel-to-backwater entrance width ratios (B/b) of 2 and 10 were simulated. Main-channel-to-backwater-depth ratios (D/d) were varied from 1 to 4 . Sketches of these geometries followed by the corresponding time-histories of the drawdown and currents generated by the vessel passage are shown in Plates 110-133. The main channel stations are located in the main channel

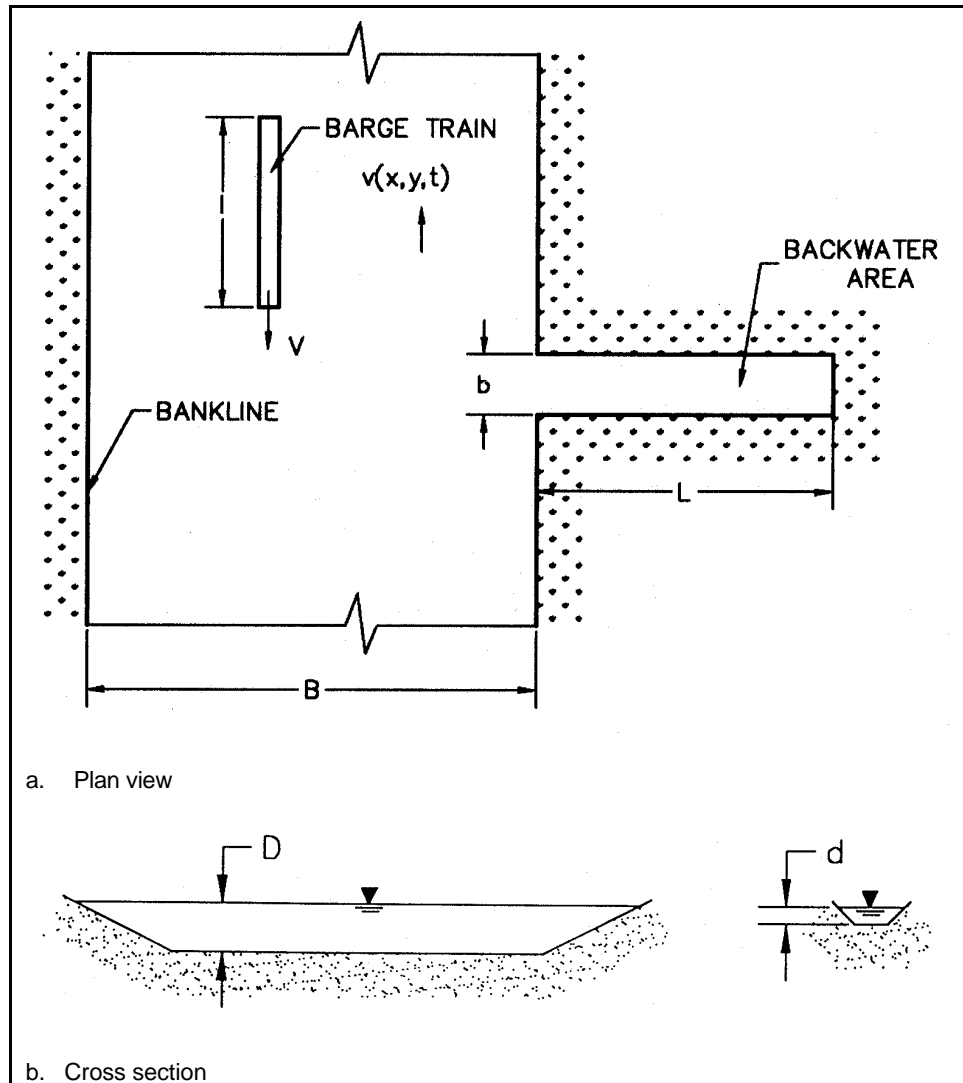


Figure 6. Geometric and hydraulic parameters describing backwaters

adjacent to the island center at a point one-half the distance from the sailing line to the island.

The depression caused by this vessel-generated pulse in a backwater initially causes a pulse of flow from the backwater channel into the main stem. This depression travels upstream until it is reflected off the closed end of the backwater. The reflected pulse is a depression, but the velocity is now directed into the backwater, toward the closed end. This reflected wave will then travel to the main stem. When the wave reaches the main stem, the junction of the main stem and backwater behaves like a reservoir so that the water surface will remain a constant but the velocities will be amplified. In some cases, the results will show larger velocity magnitudes at this point than from the initial drawdown velocity. So the reflection at the junction of the main stem and the backwater represents an overshoot in which the reflection of the depression wave is a positive wave traveling back into the

backwater. A complete cycle requires the wave to travel the length of the backwater channel four times. This is a period of $4L/(gH)^{1/2}$, where L is the channel length. The sum of the wave and its reflection produces a standing wave in the backwater. Here the water surface through the backwater will rise and fall in phase. The velocity will be out of phase with the water-surface wave. This is apparent in the plates for the backwater with length $L/l = 1$. The largest velocity amplitude is found at the entrance, and the largest water-surface amplitude is at the closed end of the backwater.

6 Discussion and Conclusions

Discussion

The numerical model is an effective tool for quantifying the flow conditions in a navigation channel due to a moving tow traveling a predetermined sailing line. Velocities and water-surface fluctuations calculated using the depth-averaged flow equations provide a detailed determination of the magnitude and distribution of the flow field. Time-history comparisons capture the magnitude, flow reversals, and timing of these phenomena.

Advantages of this method over traditional one-dimensional analytical approaches for the quantification of tow-induced current and drawdown are many. Solution of the energy and continuity equations, as presented by Jansen and Schijf (1953), provides only a cross-sectional average return current and drawdown at midship in a uniform channel. The numerical model generates wave movement and gradients in two dimensions in a channel of arbitrary shape. The numerical model can be used to evaluate scenarios that are difficult to measure in the field or in a physical model. These scenarios include two tows passing and tows navigating channel bends. Finally, the numerical model provides visualization products that enable understanding of the complicated effects produced by vessels moving in a navigation channel.

Conclusions

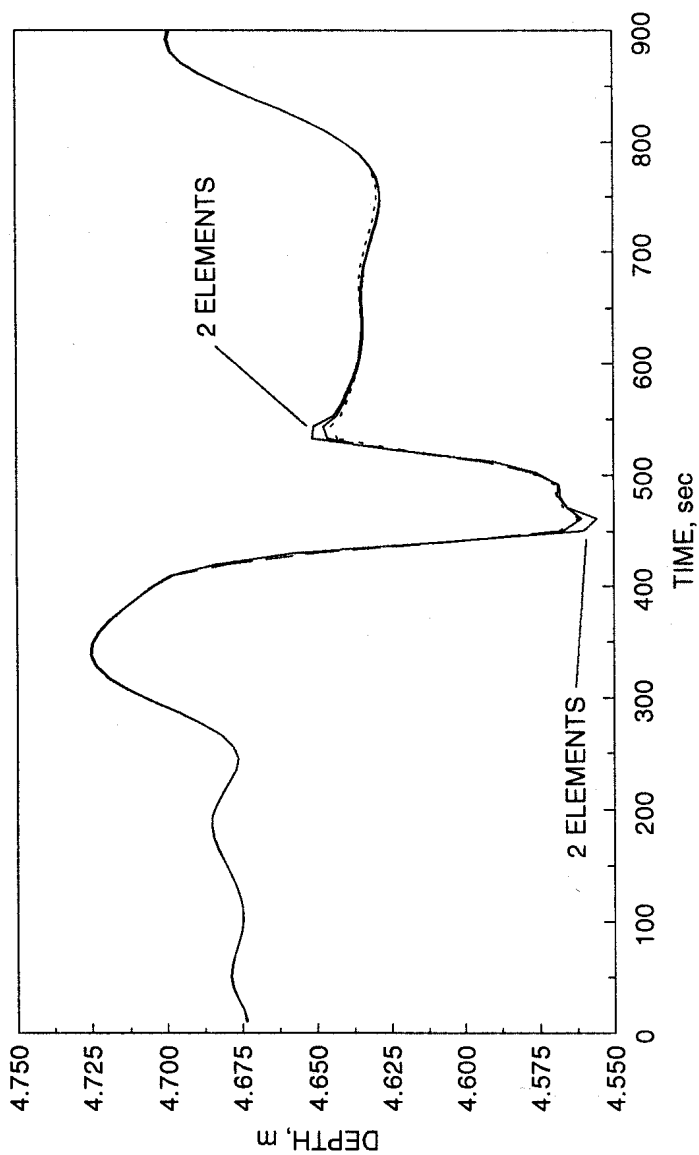
The model is limited to flows that are adequately described by the shallow-water equations; that is, three-dimensional flow near the vessel, where the vertical accelerations are significant, is not simulated. Vertical acceleration beneath the bow and stern may be so great that the shallow-water model is not applicable to the flow beneath the vessel. Another limitation of shallow-water models is that they cannot simulate short-period waves composing the divergent and stern wave field produced by a moving vessel. Also, no attempt has been made to reproduce the effects of a towboat propeller jet.

The shallow-water equations coupled with a moving pressure field representing the displacement of a vessel effectively model the far-field (area greater than about 2 to 2.5 vessel widths from the sailing line) currents and drawdown produced by a tow in an irregular channel section. The results of the "blind" tests comparing the physical model and prototype measurements to the numerical model calculations support this conclusion.

References

- Abbott, M. B. (1979). *Computational hydraulics, elements of the theory of free surface flows*, Pitman Advanced Publishing Limited, London, 43.
- Berger, R. C. (1993). "A finite element scheme for shock capturing," Technical Report HL-93-12, U.S. Army Engineer Waterways Experiment Station, Vicksburg, MS.
- Berger, R. C., and Stockstill, R. L. (1995). "Finite-element model for high-velocity channels," *Journal of Hydraulic Engineering* 121(10), 710-716.
- Bhowmik, N. G., Soong, T. W., and Xia, R. (1993). "Physical effects of barge tows on the Upper Mississippi River System: Analysis of existing data collected by the Illinois Water Survey from the Kampsville Site on the Illinois River," Draft Progress Report No. 2, Illinois State Water Survey, Champaign, IL.
- _____. (1994). "Physical effects of barge tows on the Upper Mississippi River System: Analysis of existing data collected by the Illinois water survey from the Clark's Ferry site on the Mississippi River," Draft Progress Report, Illinois State Water Survey, Champaign, IL.
- Brater, E. F., and King, H. W. (1976). *Handbook of hydraulics for the solution of hydraulic engineering problems*. McGraw-Hill, New York. 7-17.
- Chapman, R. S., and Kuo, C. Y. (1985). "Applications of the two-equation $k-\epsilon$ turbulence model to a two-dimensional, steady, free surface flow problem with separation," *International Journal for Numerical Methods in Fluids* 5, 257-268.
- Jansen, P. Ph., and Schijf, J. B. (1953). *18th International navigation congress*, Rome. Permanent International Association of Navigation Congresses, Brussels, Section 1, Communication 1, 175-197.
- Katopodes, N. D. (1986). "Explicit computation of discontinuous channel flow," *Journal of Hydraulic Engineering*, ASCE, 112(6), 456-475.

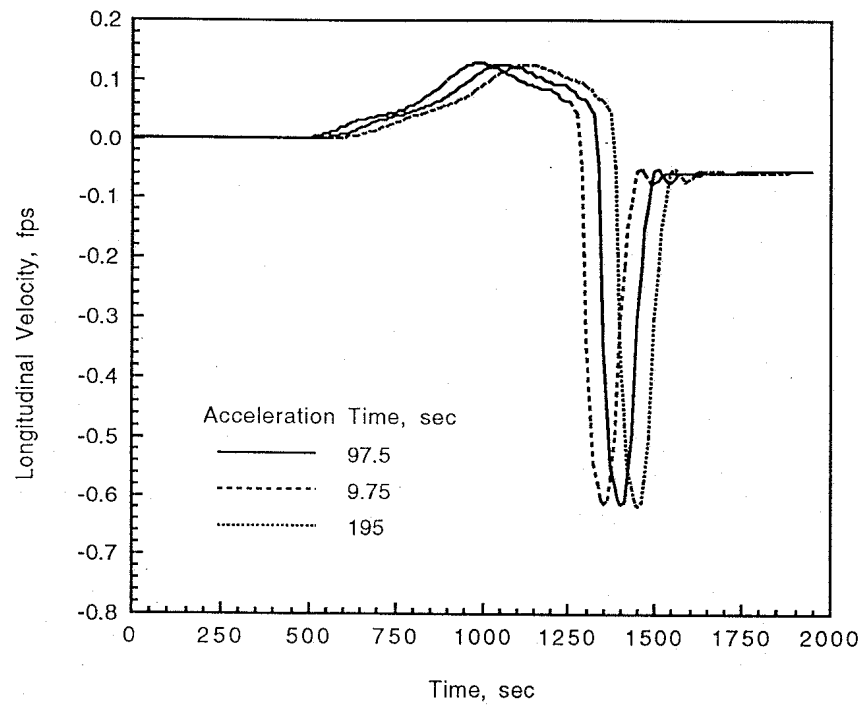
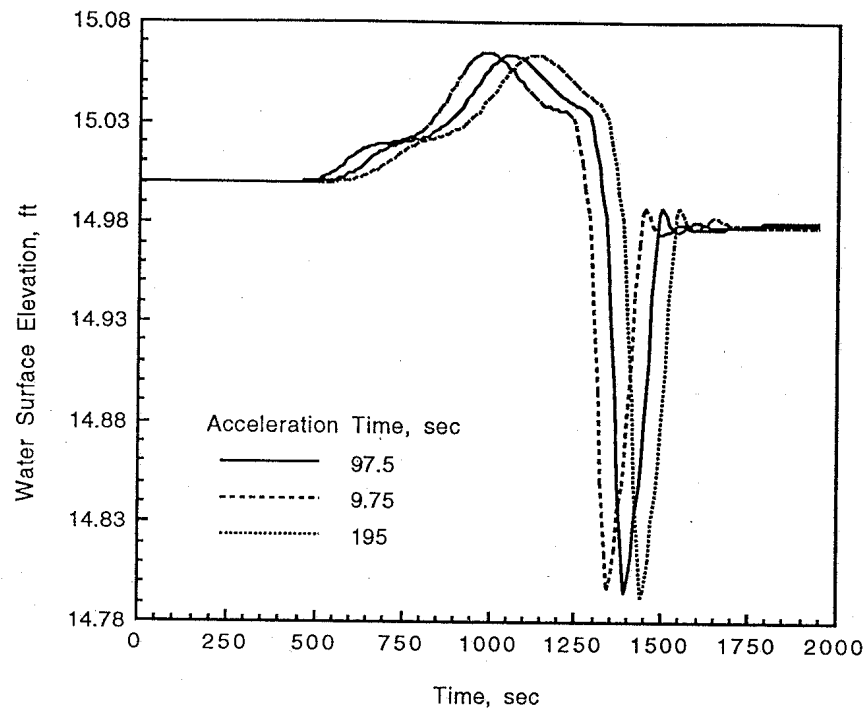
- Maynard, S. T. (1996). "Return velocity and drawdown in navigable waterways," Technical Report HL-96-7, U.S. Army Engineer Waterways Experiment Station, Vicksburg, MS.
- Maynard, S. T., and Martin, S. K. (1997). "Interim Report for the Upper Mississippi River - Illinois Waterway System Navigation Study, Physical Forces Study, Kampsville, Illinois Waterway," ENV Report 3, U. S. Army Engineer Waterways Experiment Station, Vicksburg, MS.
- Maynard, S. T., and Martin, S. K. (1998). "Interim Report for the Upper Mississippi River - Illinois Waterway System Navigation Study, Physical Forces Study, Clark's Ferry, Mississippi River," ENV Report 5, U. S. Army Engineer Waterways Experiment Station, Vicksburg, MS.
- Maynard, S. T., and Siemsen, T. S. (1991). "Return velocities induced by shallow-draft navigation." *Hydraulic Engineering: Proceedings of the 1991 National Conference*, Nashville, TN, July 29 – August 2, 1991. R. M. Shane, ed., ASCE, New York, 894-899.
- Rodi, W. (1980). "Turbulence models and their application in hydraulics - a state of the art review," State-of-the art paper, International Association for Hydraulic Research, Delft, The Netherlands.
- Stockstill, R. L., and Berger, R. C. (1994). "HIVEL2D: a two-dimensional flow model for high-velocity channels," Technical Report REMR-HY-12, U.S. Army Engineer Waterways Experiment Station, Vicksburg, MS.
- Stoker, J. J. (1957). *Water waves, the mathematical theory with applications*. Interscience Publishers, New York, 219-243.
- Whitham, G. B. (1974). *Linear and nonlinear waves*. John Wiley, New York, 462.



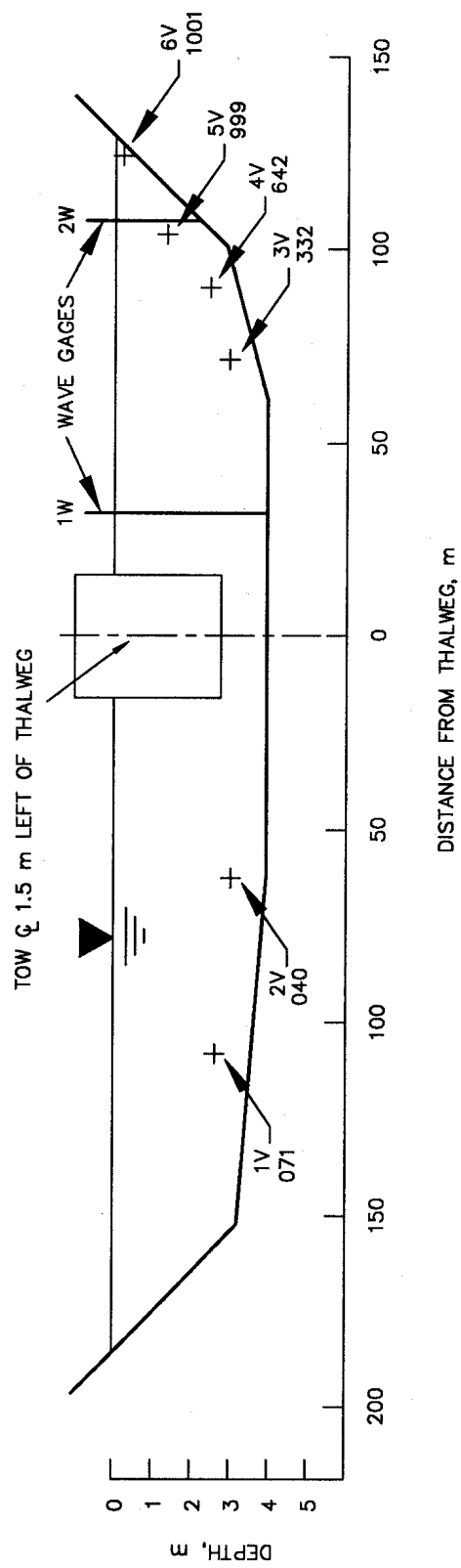
NUMBER OF ELEMENTS ACROSS VESSEL

— 2 ELEMENTS — - 3 ELEMENTS . . . 4 ELEMENTS

MESH REFINEMENT RESULTS
HYDRODYNAMIC RESPONSE AT
2.25 VESSEL WIDTHS
RIGHT OF SAILING LINE

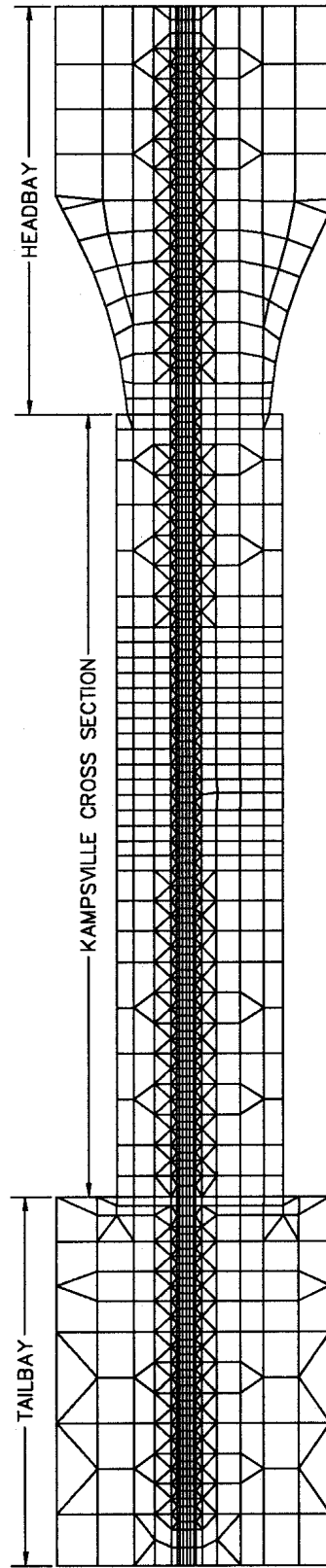


HYDRODYNAMIC RESPONSE AT
TOP OF SLOPE FOR
VARIOUS ACCELERATION RATES

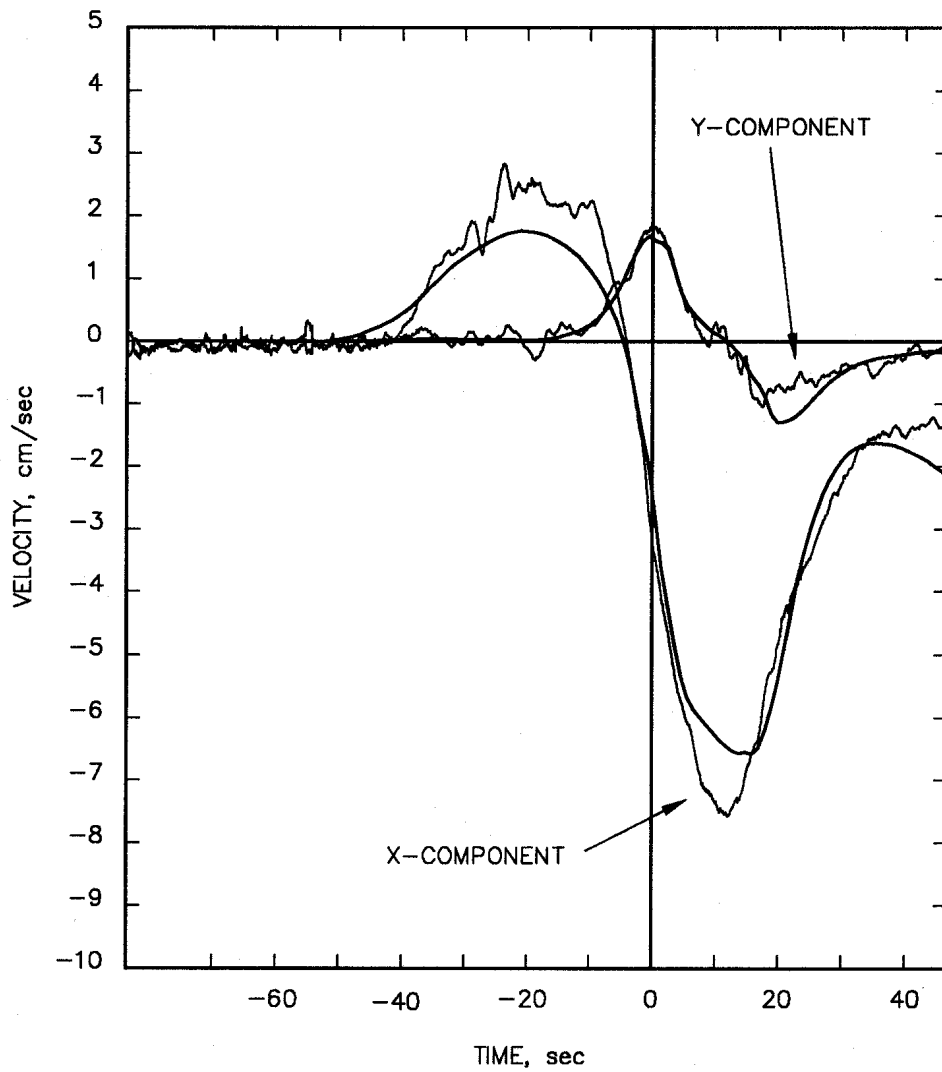


LABORATORY PROBE NUMBER	FIELD PROBE NUMBER
1V	071
2V	040
1W	—
3V	332
4V	642
5V	999
2W	—
6V	1001

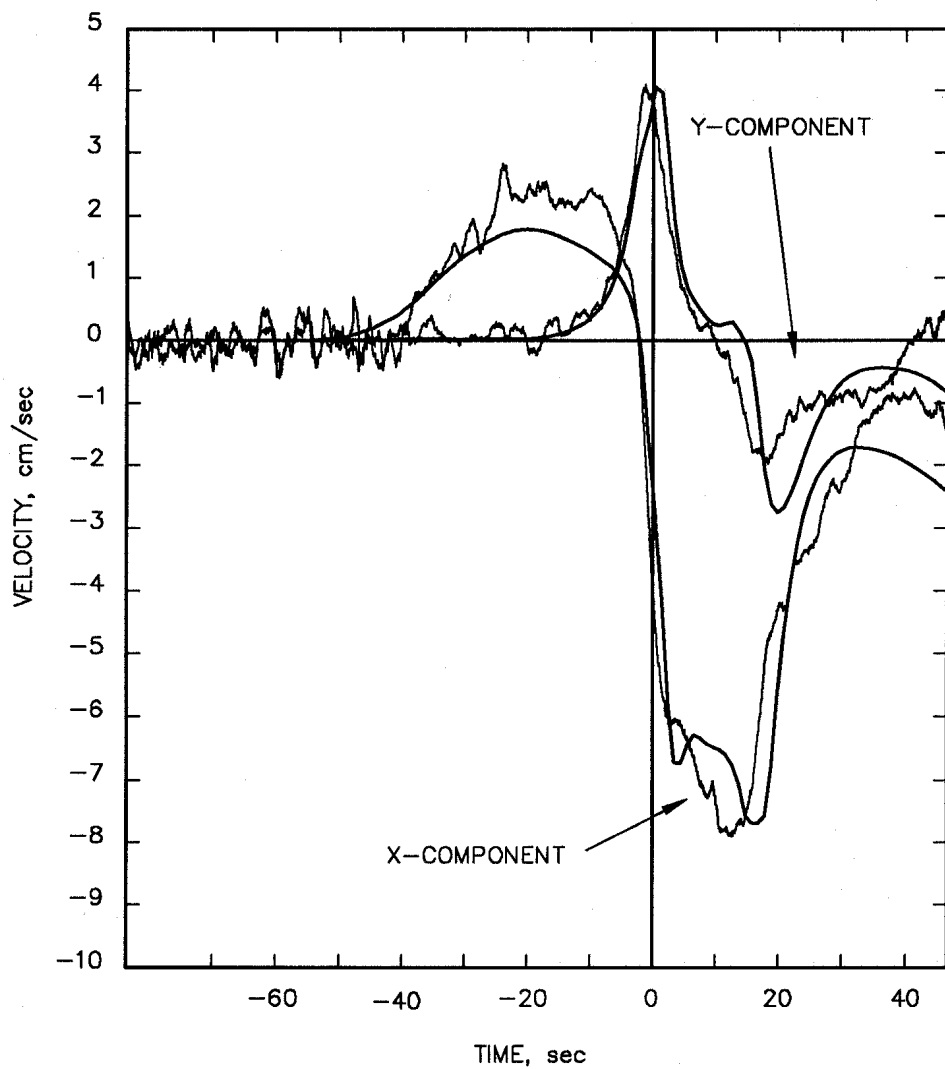
KAMPSVILLE SITE
RIVER CROSS SECTION
AND BARGE LOCATION



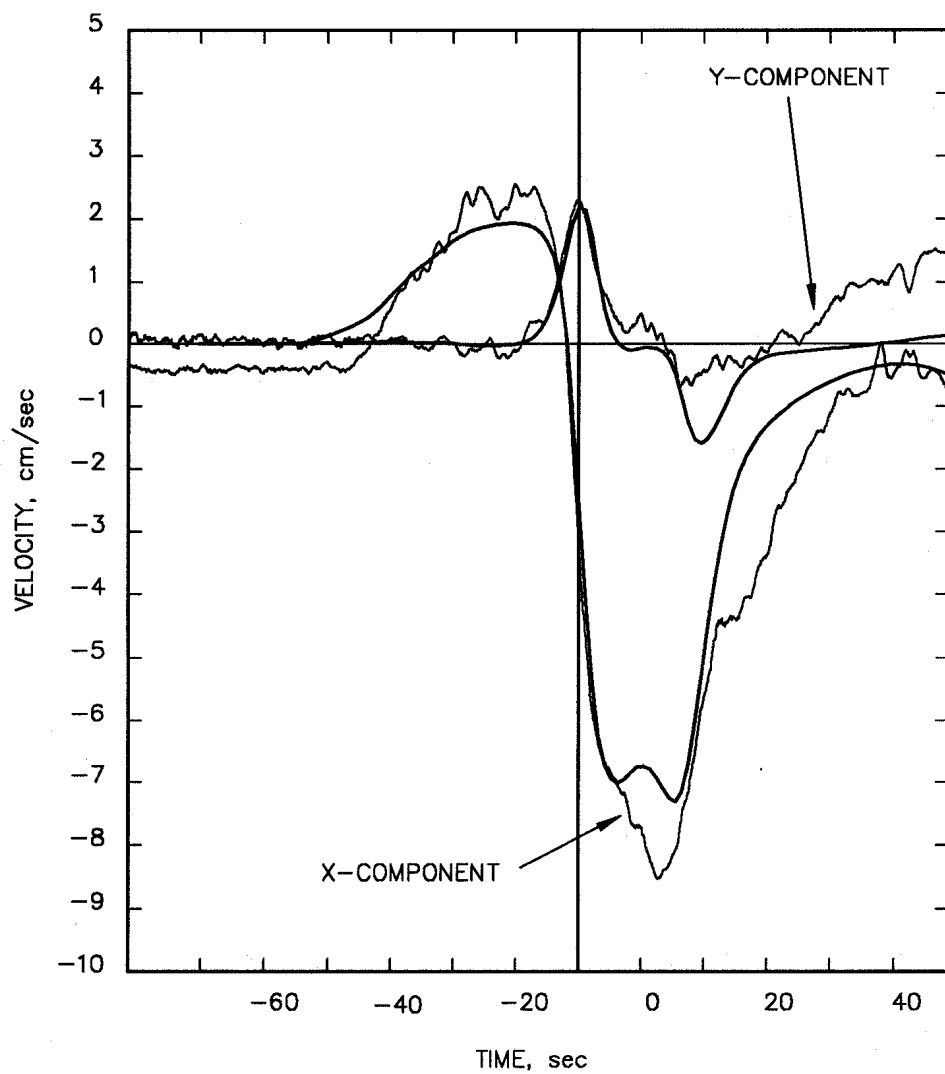
KAMPSVILLE SITE LABORATORY FLUME
NUMERICAL MODEL COMPUTATIONAL MESH



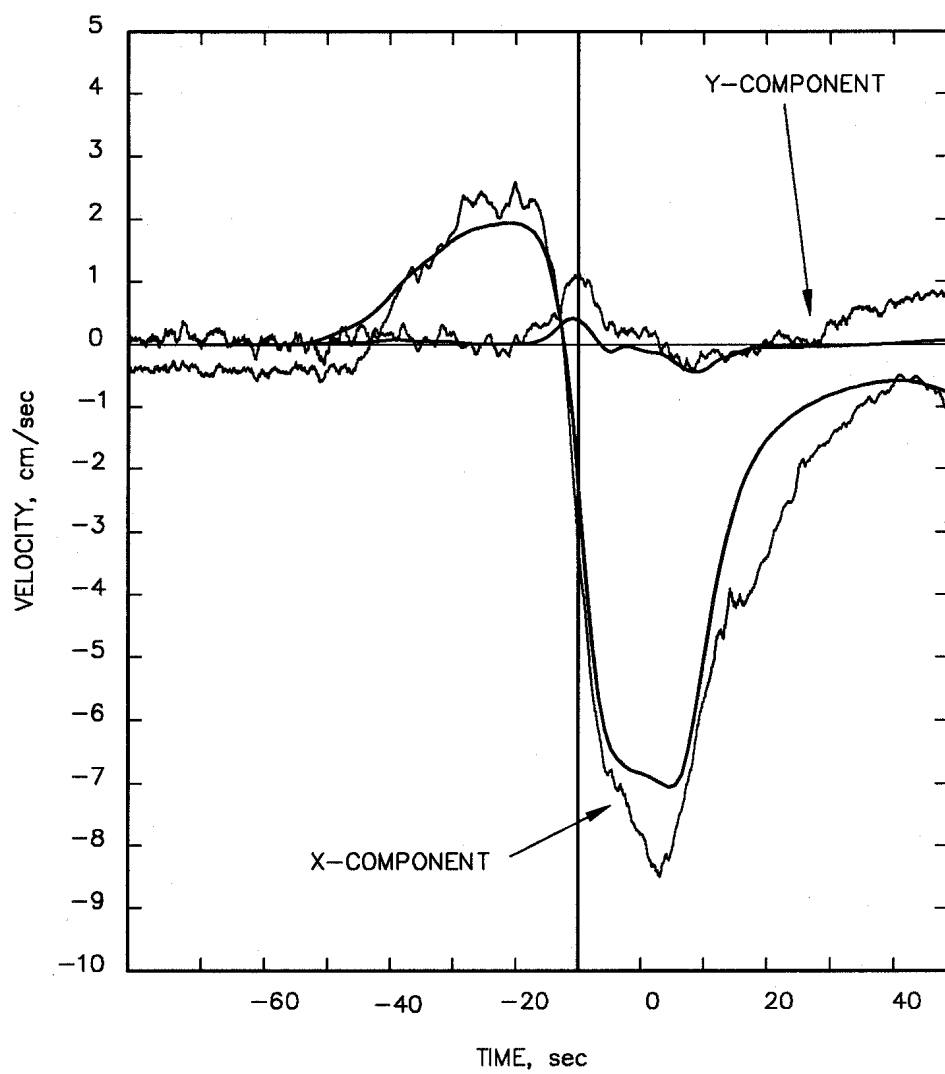
KAMPSVILLE SITE
COMPUTED AND OBSERVED VELOCITIES
PHYSICAL MODEL PROBE 1V



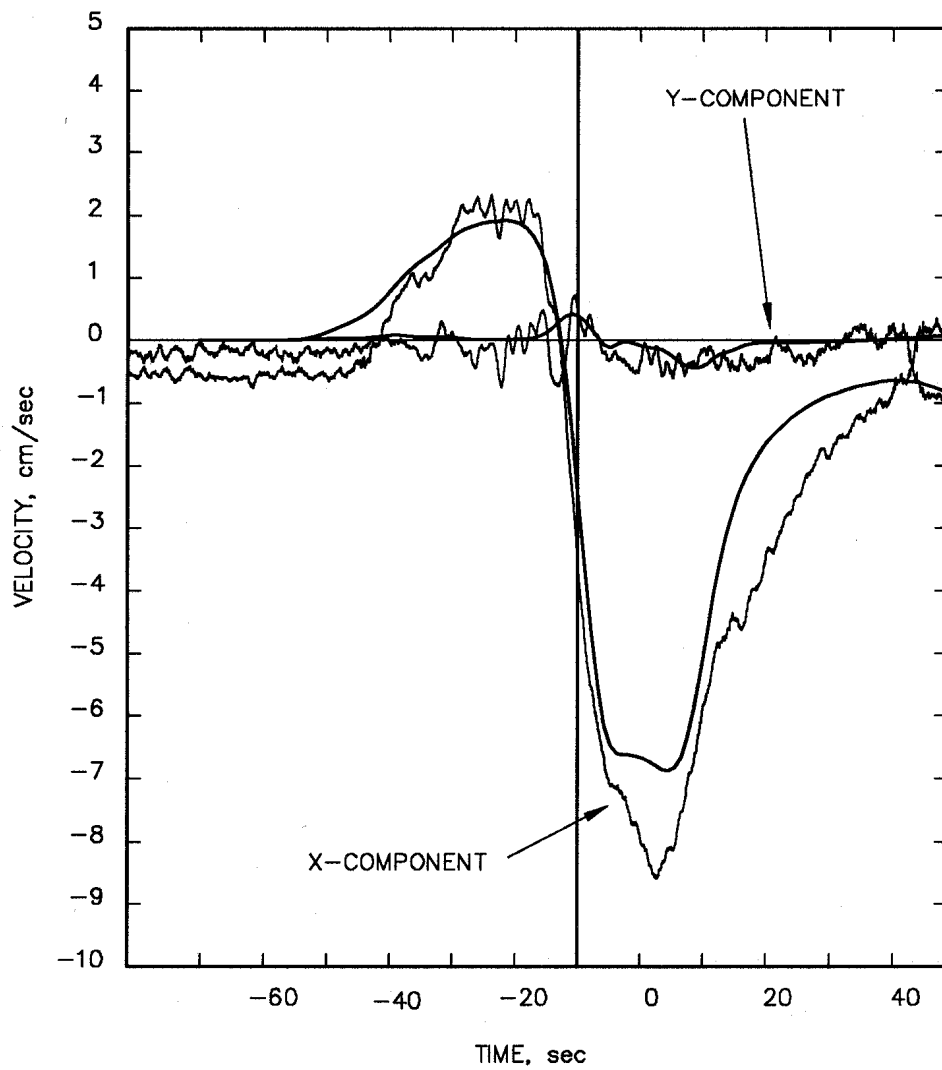
KAMPSVILLE SITE
COMPUTED AND OBSERVED VELOCITIES
PHYSICAL MODEL PROBE 2V



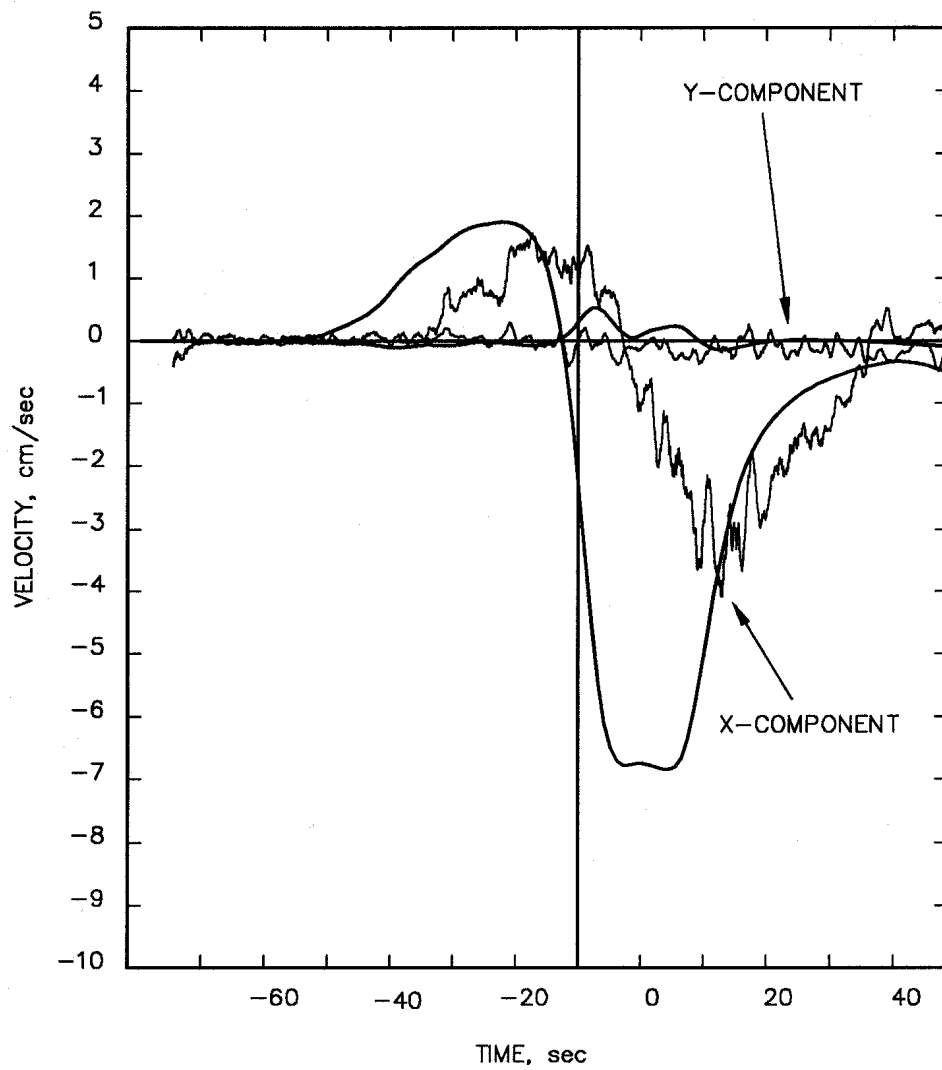
KAMPSVILLE SITE
COMPUTED AND OBSERVED VELOCITIES
PHYSICAL MODEL PROBE 3V



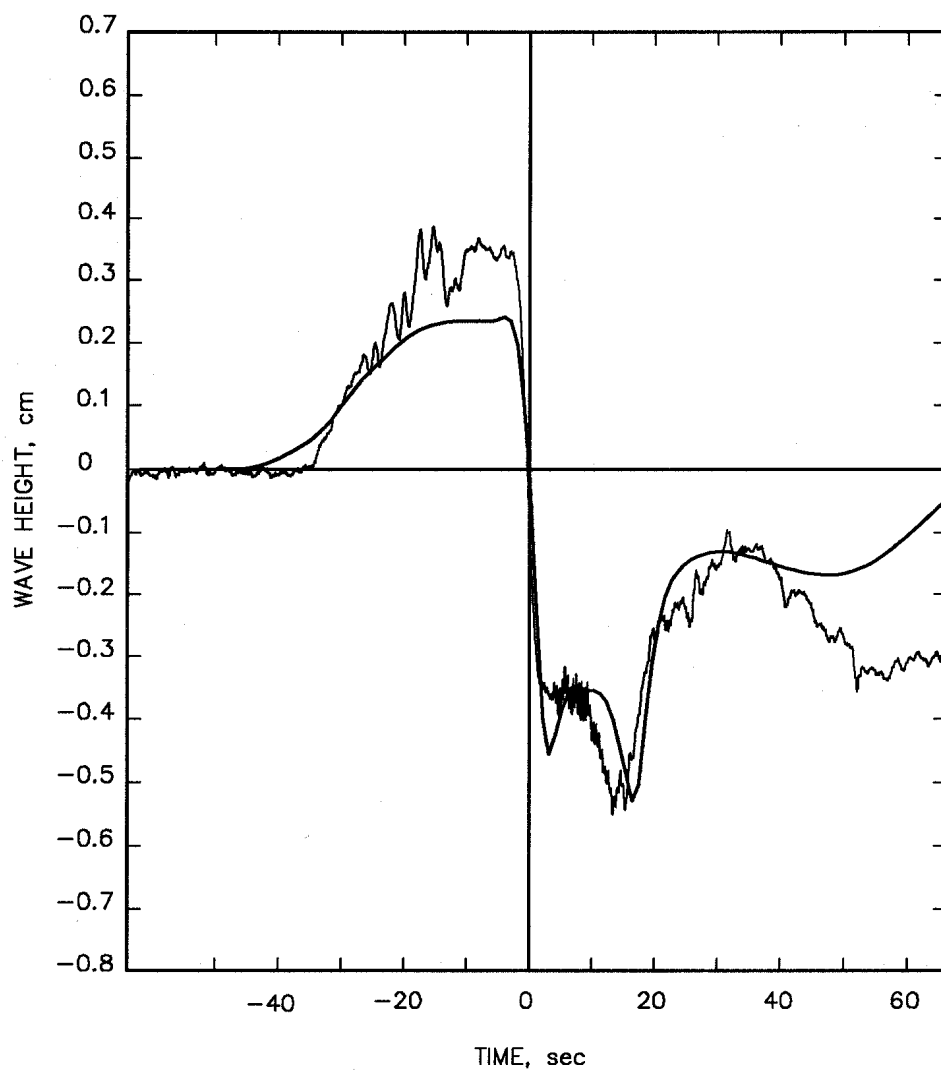
KAMPSVILLE SITE
COMPUTED AND OBSERVED VELOCITIES
PHYSICAL MODEL PROBE 4V



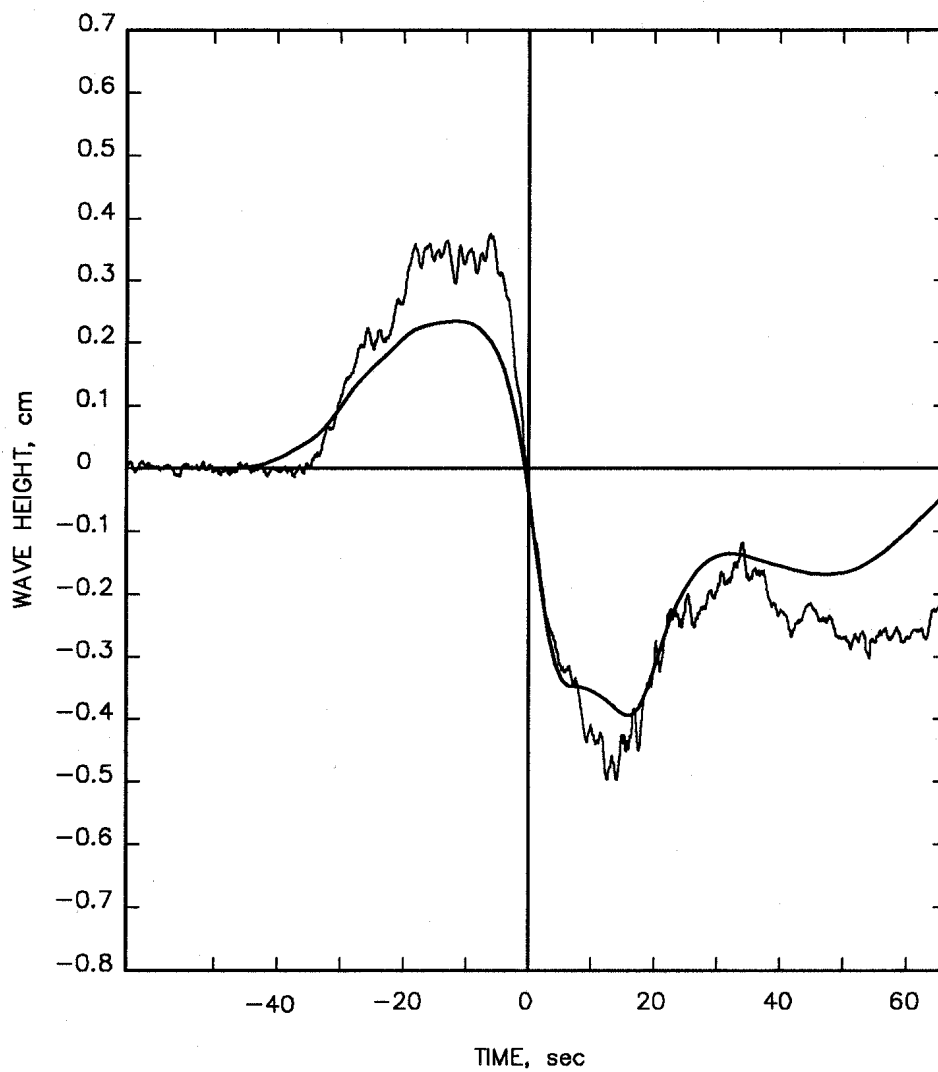
KAMPSVILLE SITE
COMPUTED AND OBSERVED VELOCITIES
PHYSICAL MODEL PROBE 5V



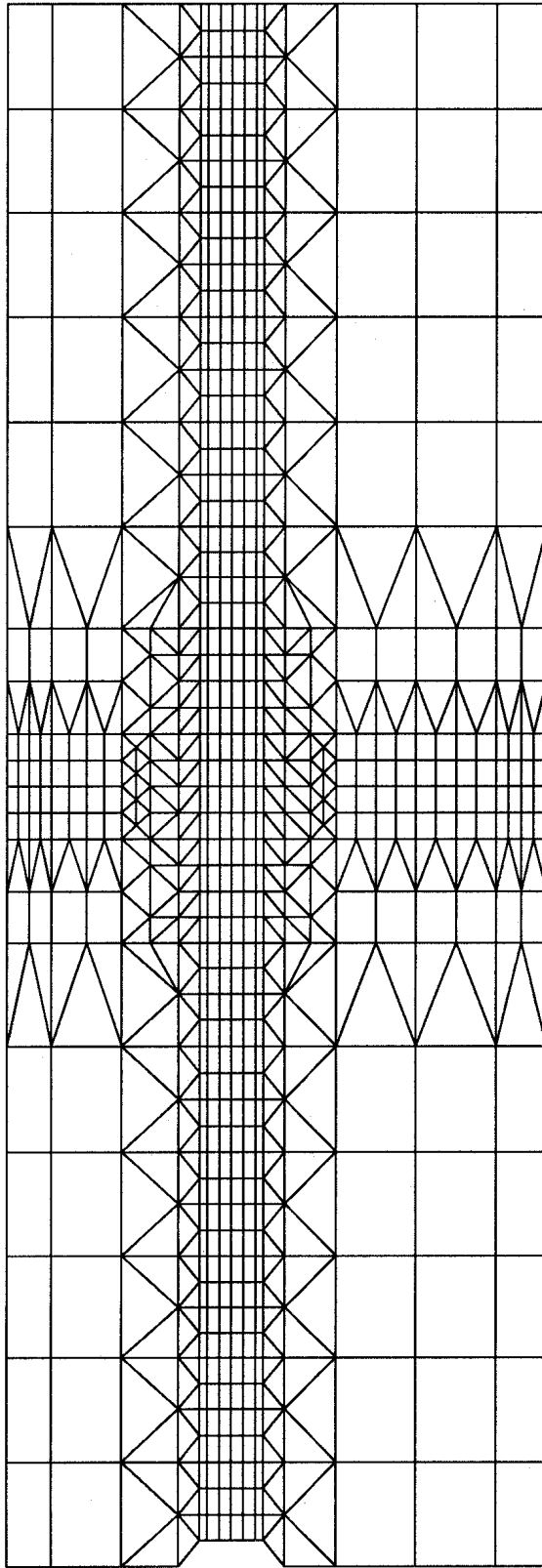
KAMPSVILLE SITE
COMPUTED AND OBSERVED VELOCITIES
PHYSICAL MODEL PROBE 6V



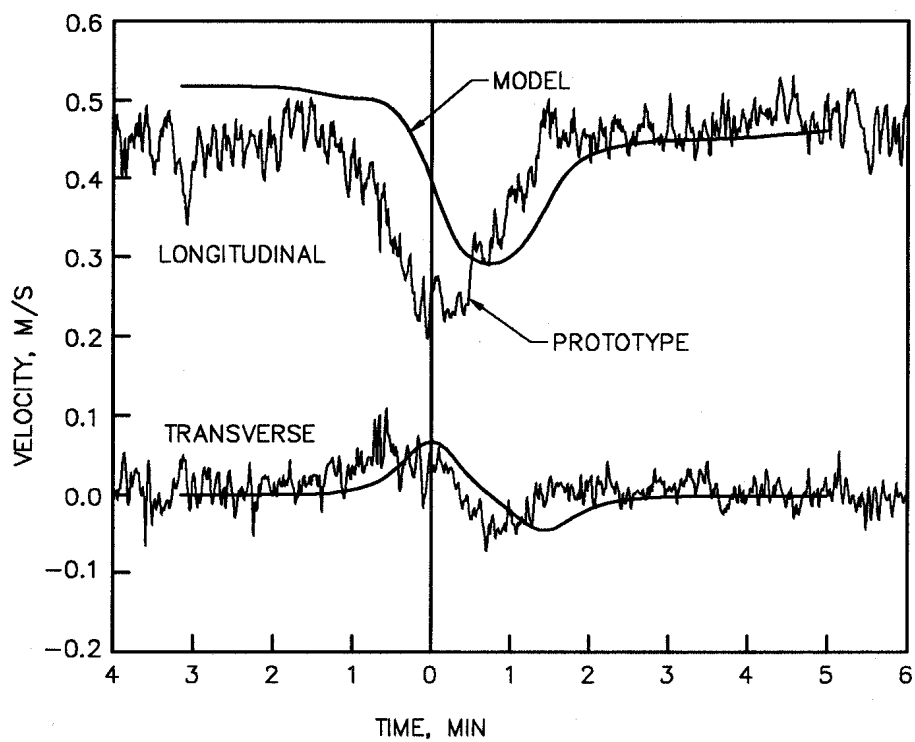
KAMPSVILLE SITE
COMPUTED AND OBSERVED WAVE HEIGHTS
RELATIVE TO STILL WATER LEVEL
PHYSICAL MODEL PROBE 1W



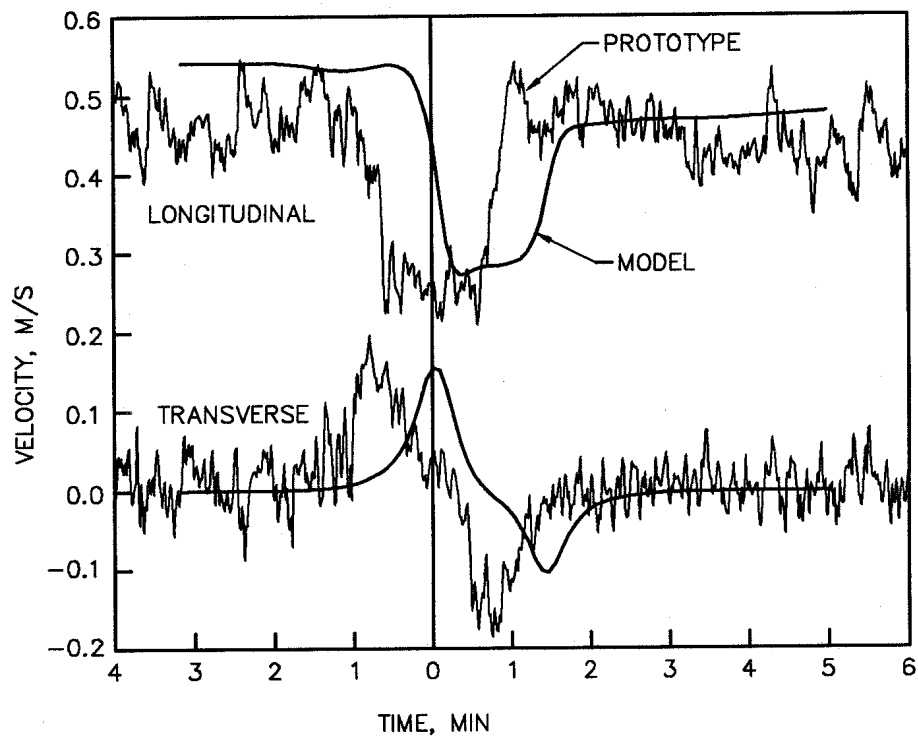
KAMPSVILLE SITE
COMPUTED AND OBSERVED WAVE HEIGHTS
RELATIVE TO STILL WATER LEVEL
PHYSICAL MODEL PROBE 2W



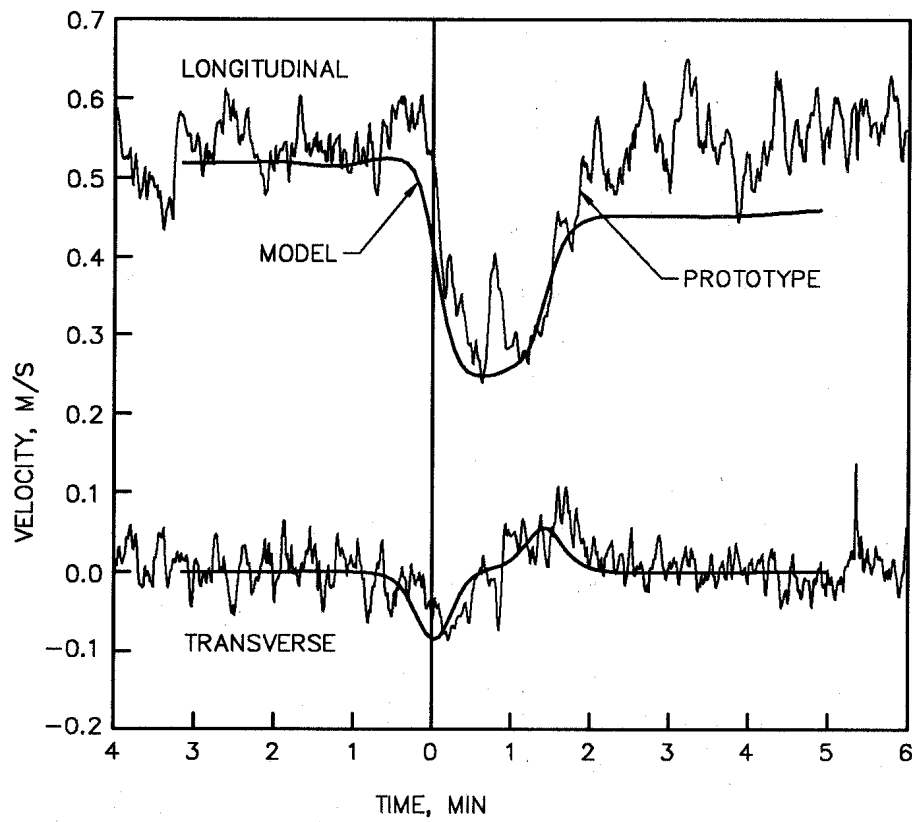
KAMPSVILLE SITE PROTOTYPE
NUMERICAL MODEL COMPUTATIONAL MESH



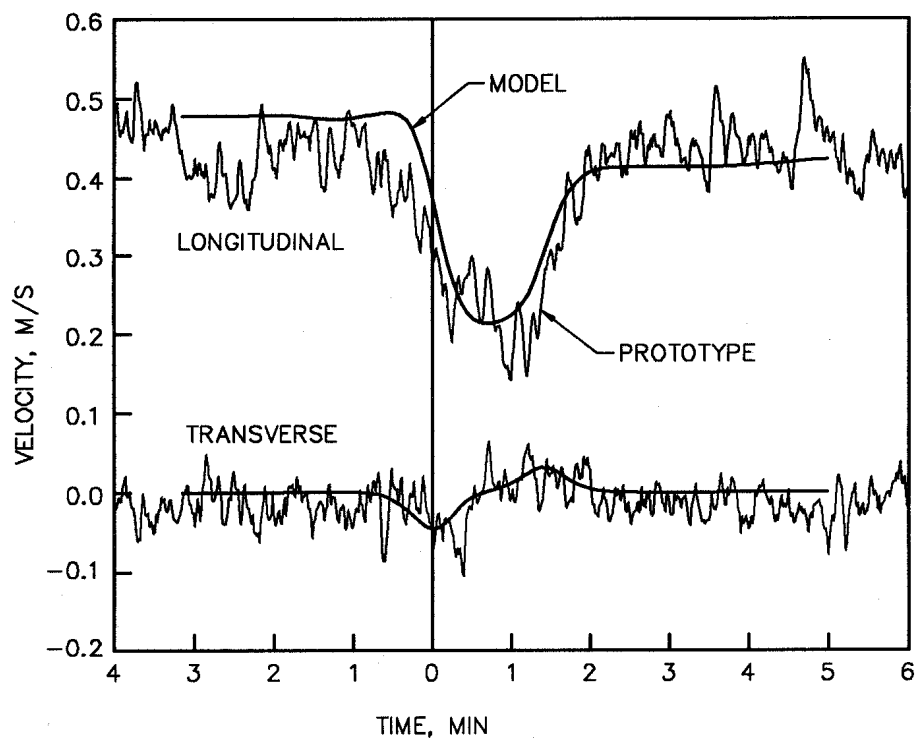
KAMPSVILLE SITE
COMPUTED AND OBSERVED VELOCITIES
PROTOTYPE GAGE 071



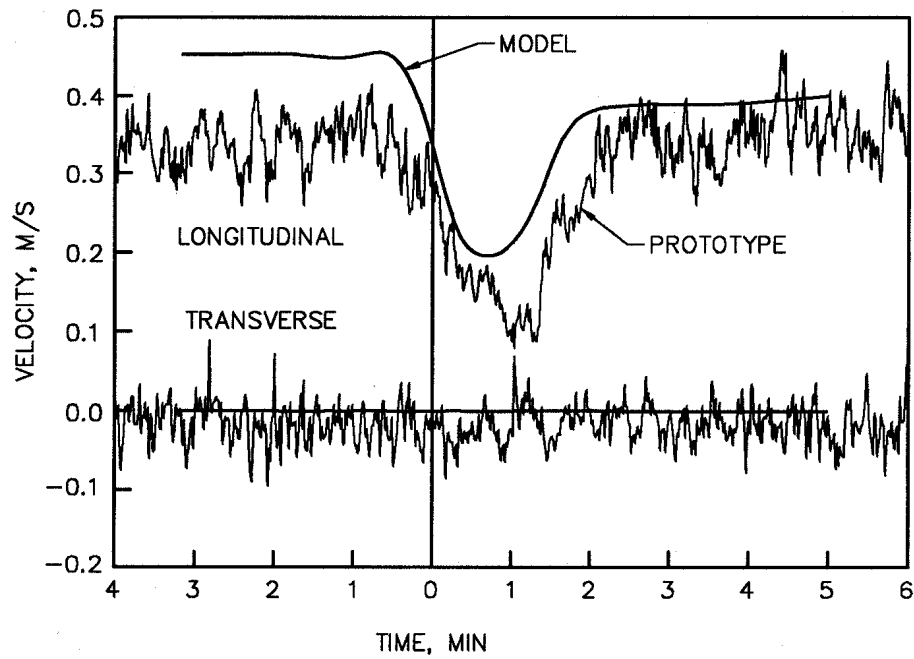
KAMPSVILLE SITE
COMPUTED AND OBSERVED VELOCITIES
PROTOTYPE GAGE 040



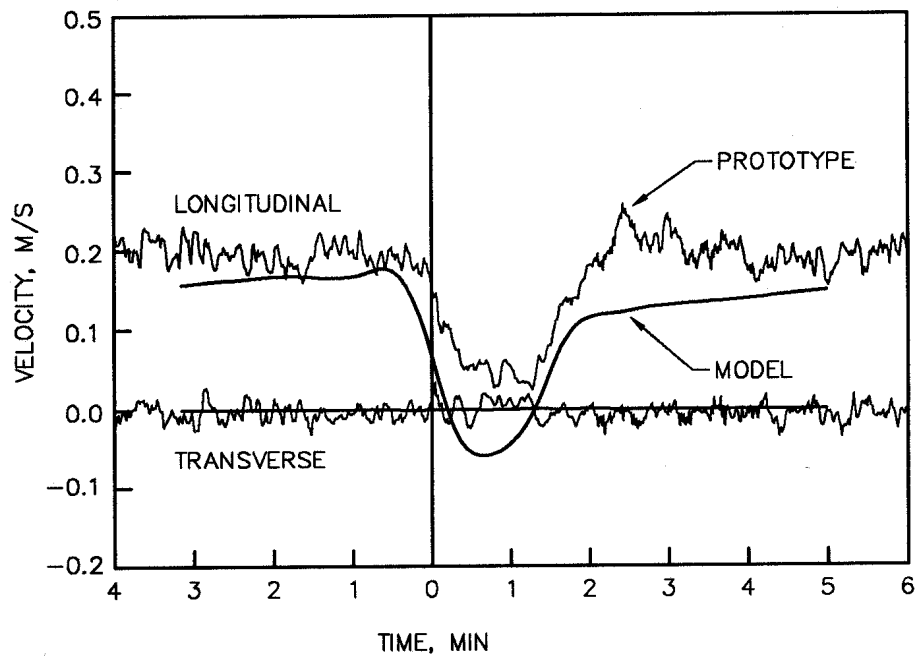
KAMPSVILLE SITE
COMPUTED AND OBSERVED VELOCITIES
PROTOTYPE GAGE 332



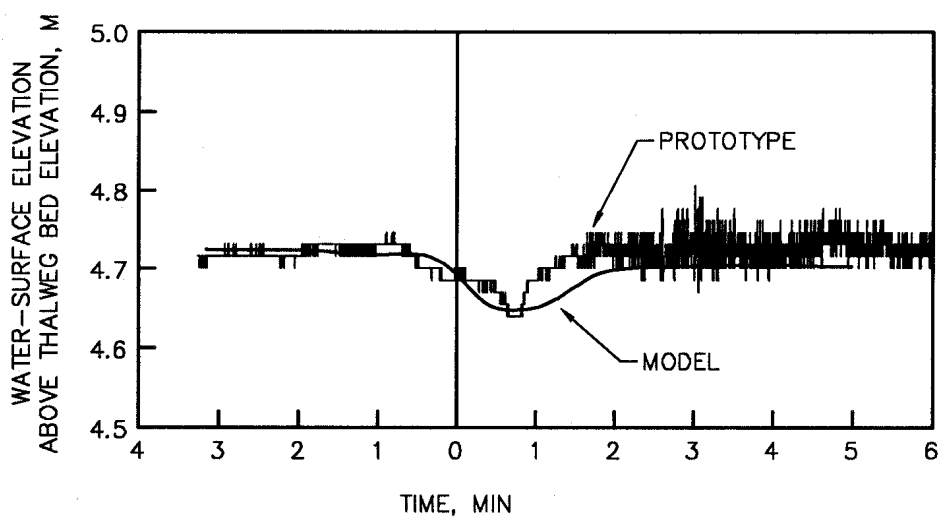
KAMPSVILLE SITE
COMPUTED AND OBSERVED VELOCITIES
PROTOTYPE GAGE 642



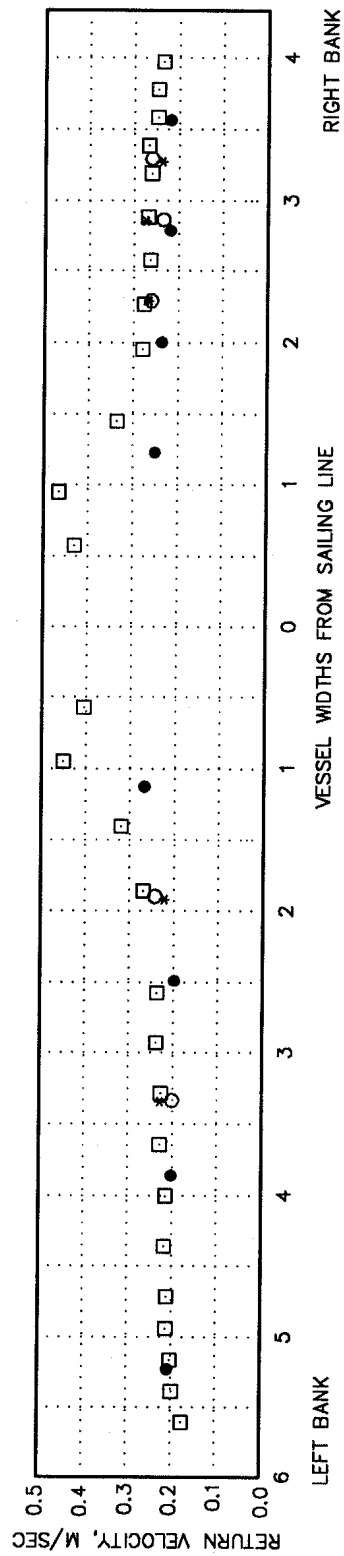
KAMPSVILLE SITE
COMPUTED AND OBSERVED VELOCITIES
PROTOTYPE GAGE 999



KAMPSVILLE SITE
COMPUTED AND OBSERVED VELOCITIES
PROTOTYPE GAGE 1001

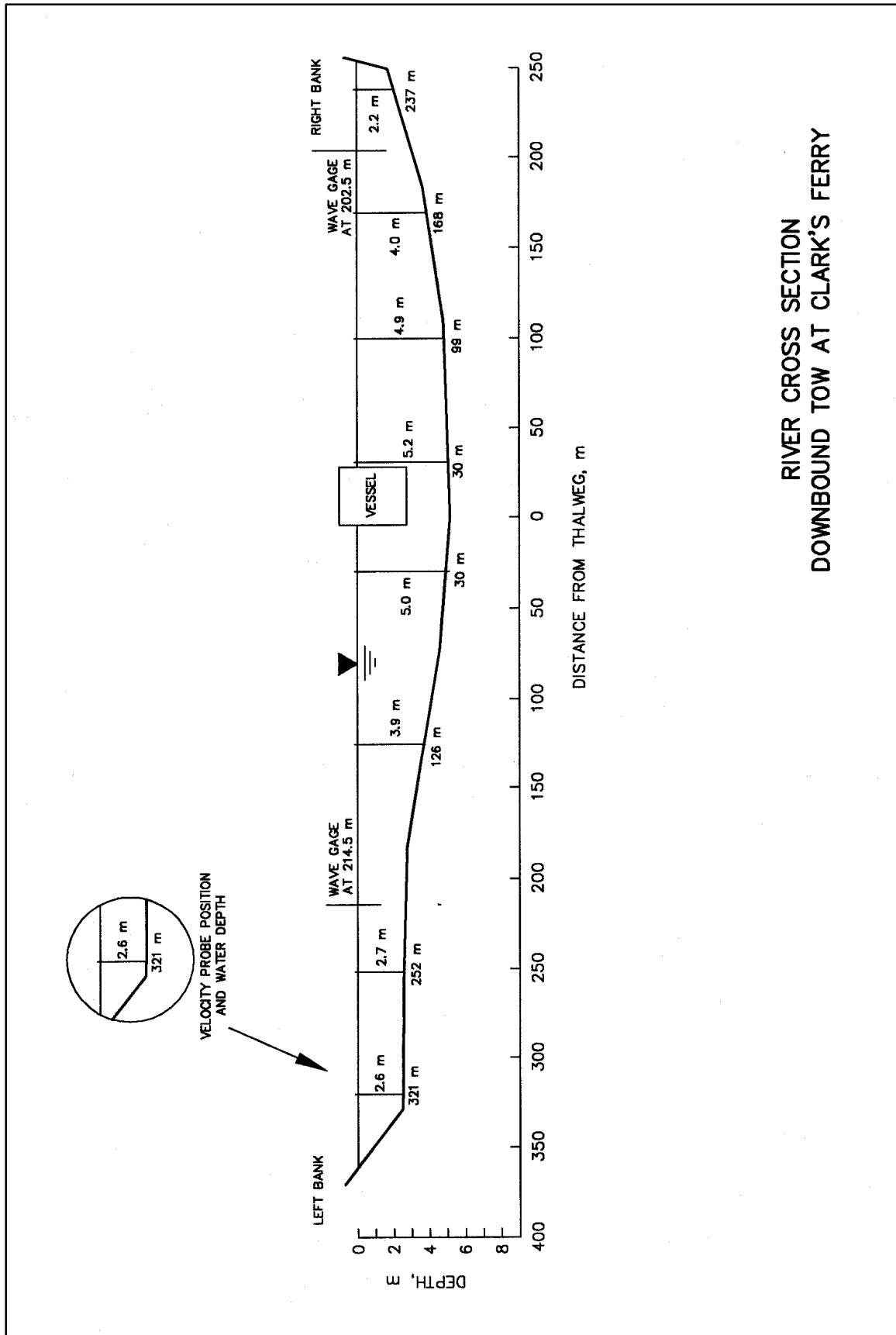


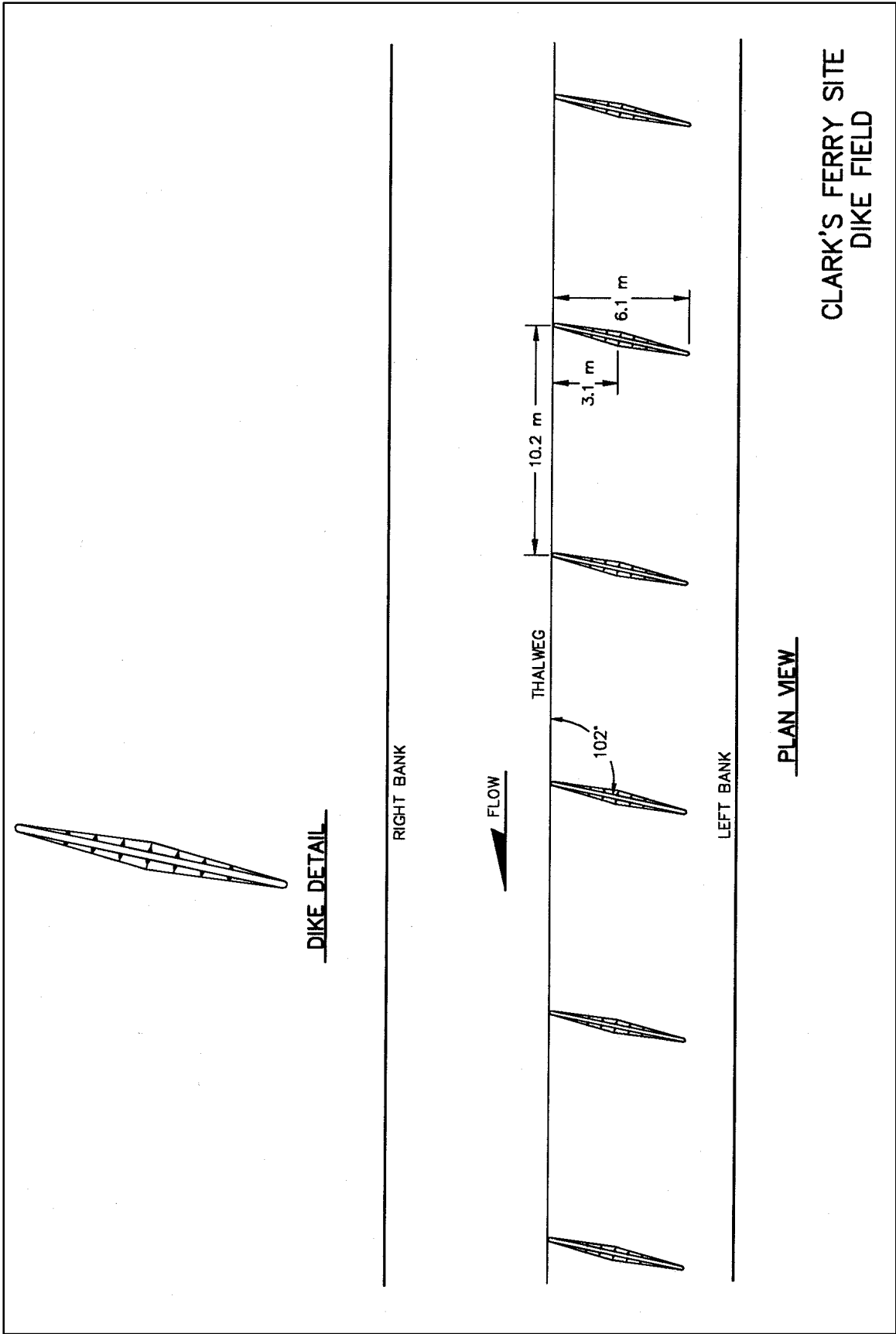
KAMPSVILLE SITE
COMPUTED AND OBSERVED
WATER-SURFACE ELEVATIONS

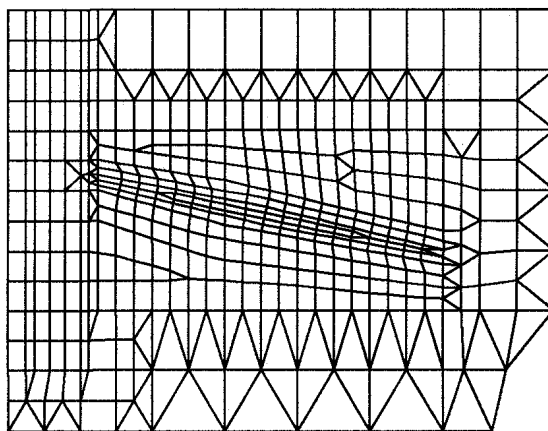
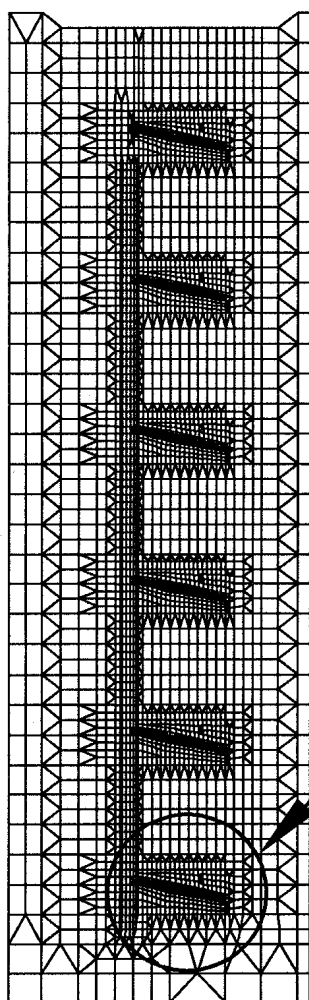


- NUMERICAL MODEL
- PHYSICAL MODEL AT 0.6*DEPTH (MAYNORD AND MARTIN 1997)
- PHYSICAL MODEL AT PROTOTYPE METER DEPTHS (MAYNORD AND MARTIN 1997)
- * PROTOTYPE (BHOWMIK, SOONG, AND XIA 1993)

RETURN CURRENT DISTRIBUTION DOWNBOUND TOW AT KAMPSVILLE

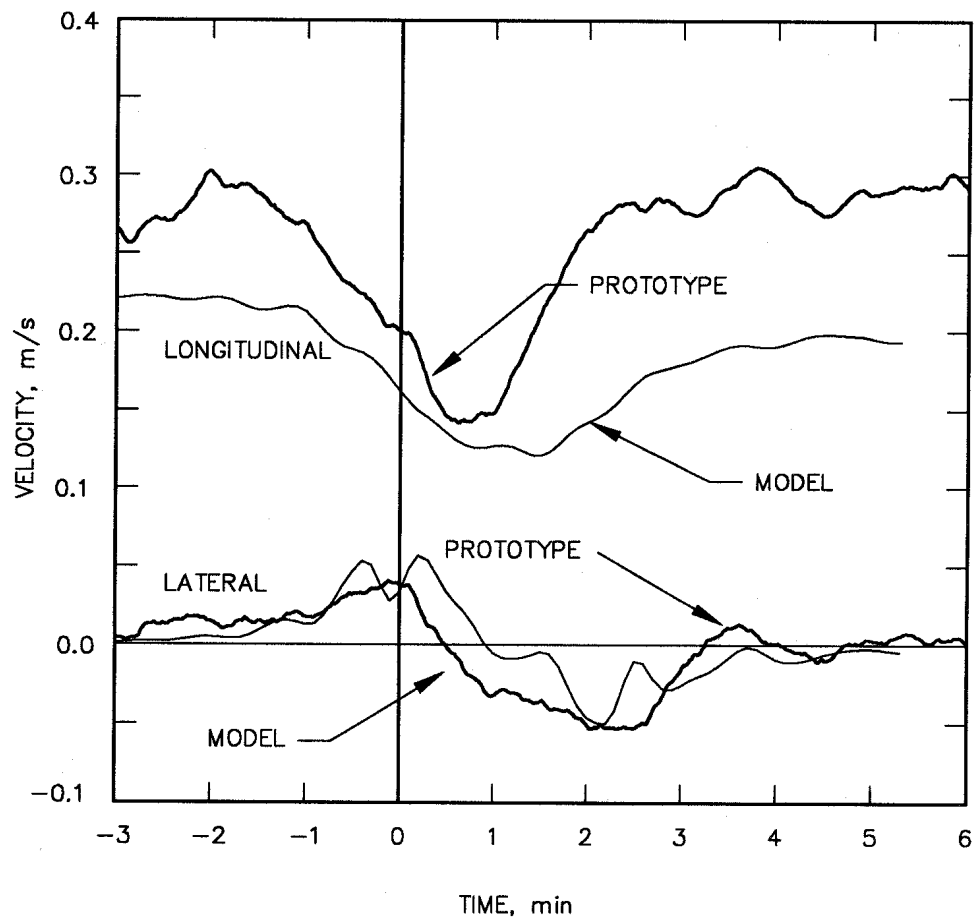




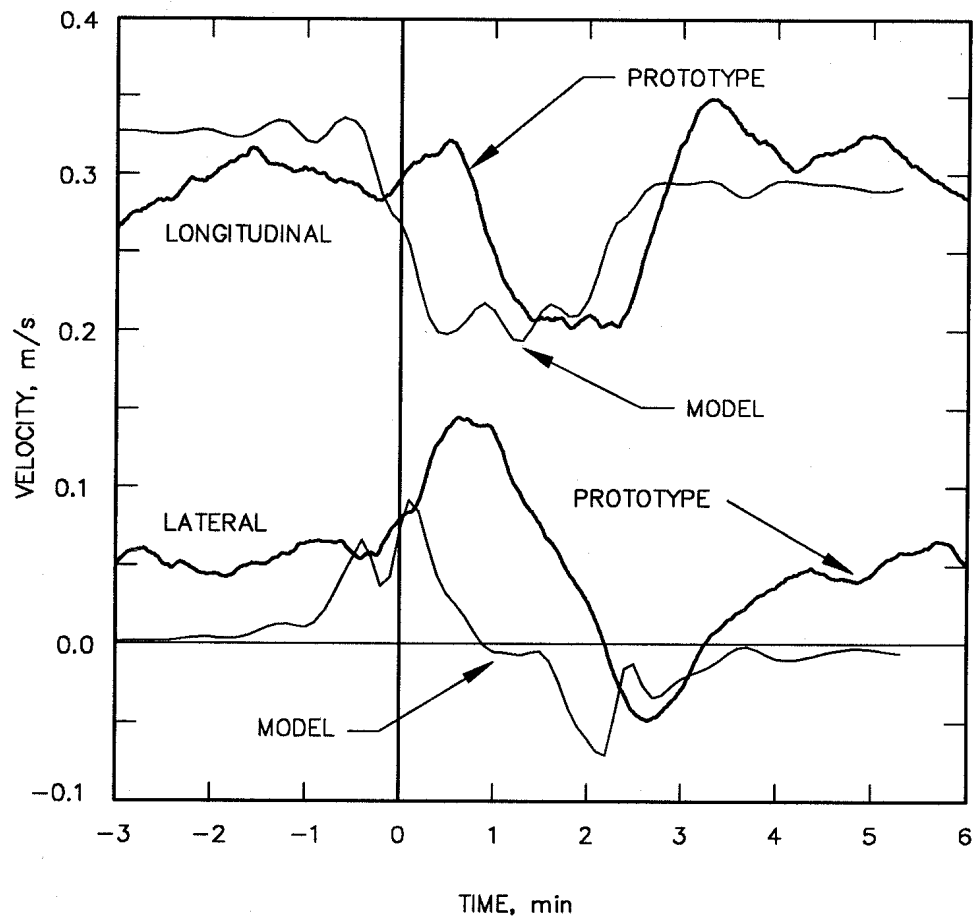


CLARK'S FERRY SITE
NUMERICAL MODEL COMPUTATIONAL MESH

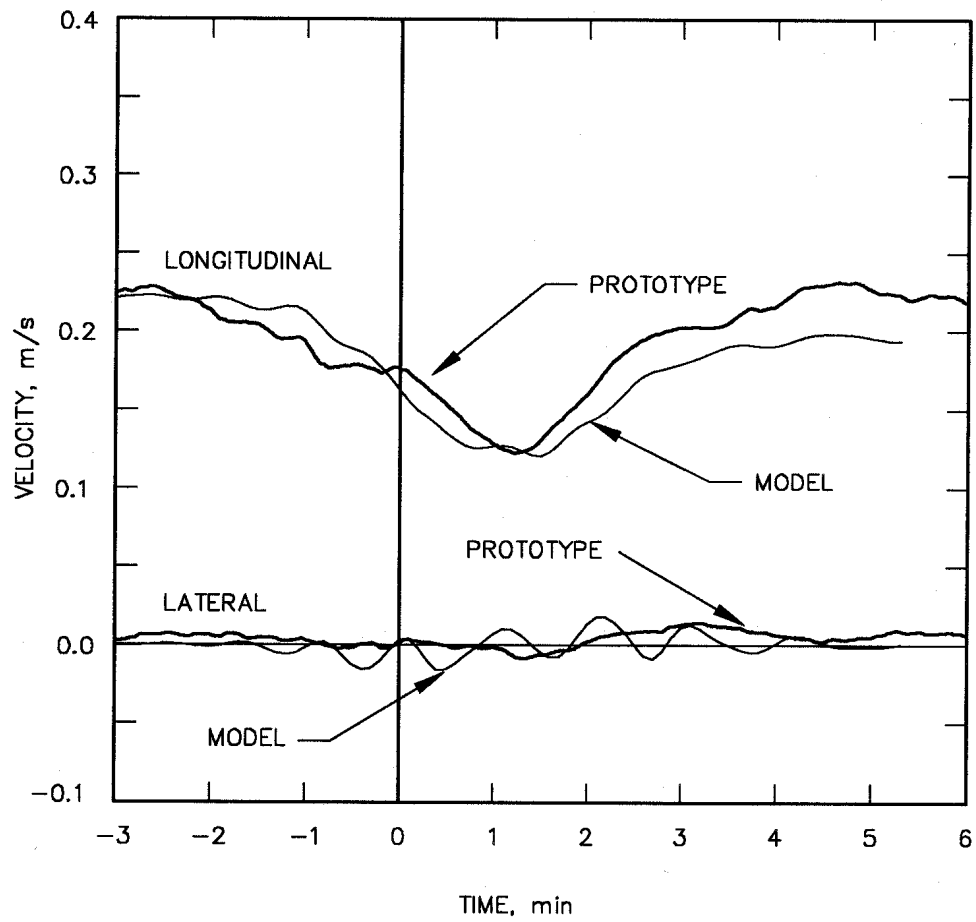
DETAILS NEAR DIKE



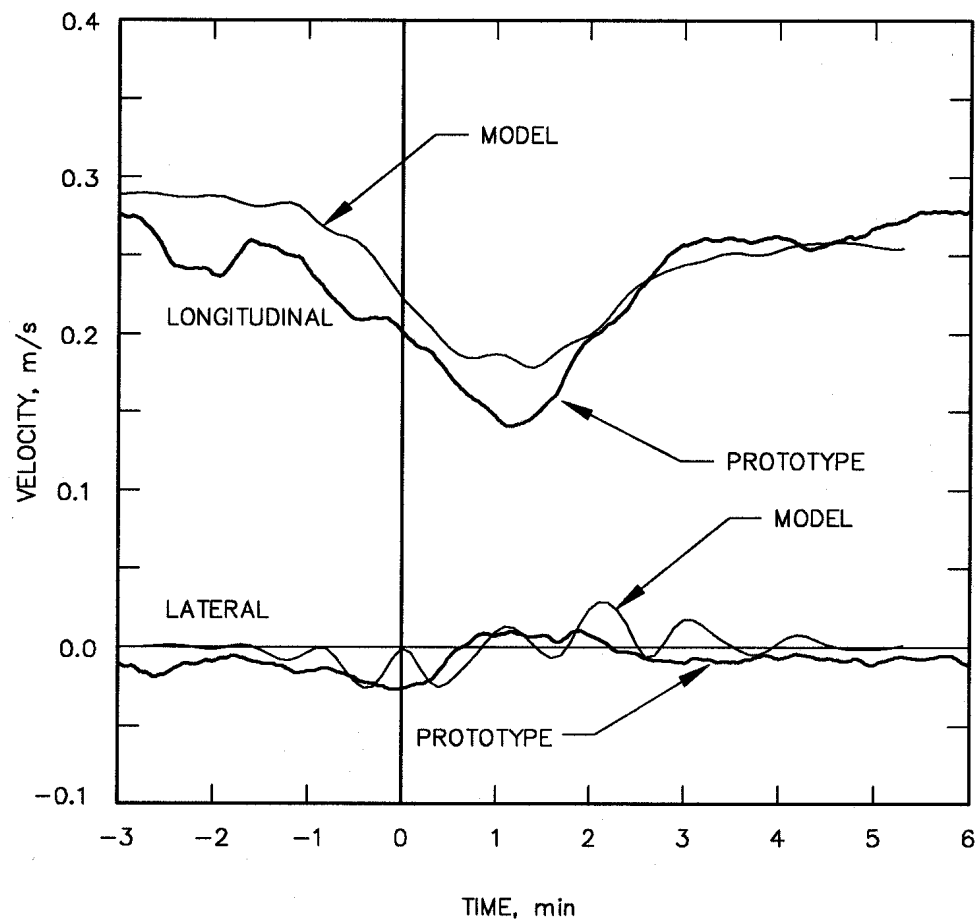
CLARK'S FERRY SITE
COMPUTED AND OBSERVED VELOCITIES
PROTOTYPE GAGE 832



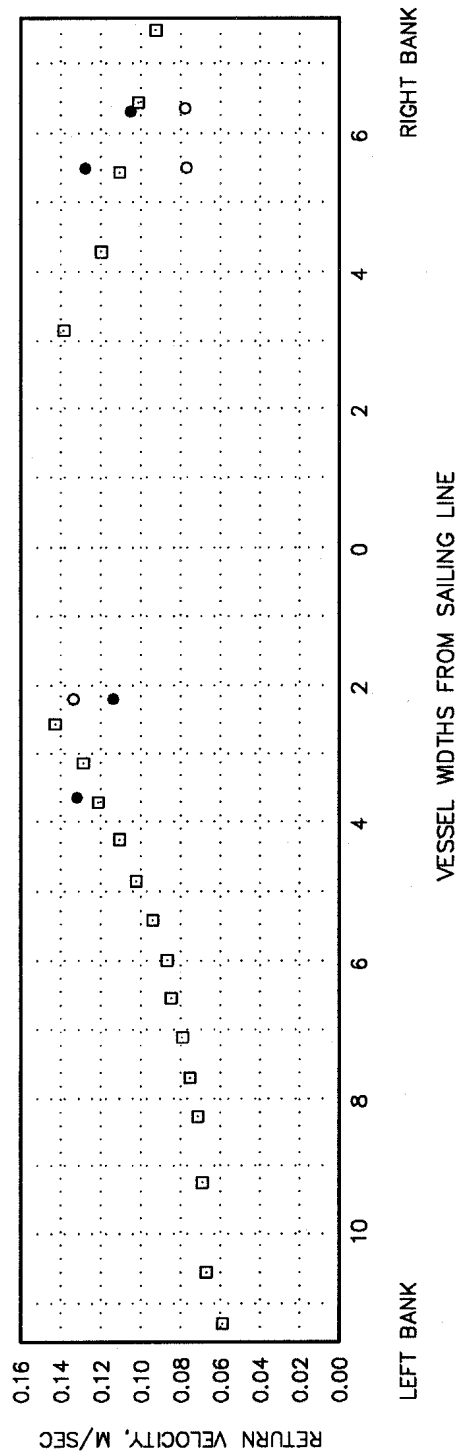
CLARK'S FERRY SITE
COMPUTED AND OBSERVED VELOCITIES
PROTOTYPE GAGE 151



CLARK'S FERRY SITE
COMPUTED AND OBSERVED VELOCITIES
PROTOTYPE GAGE 999

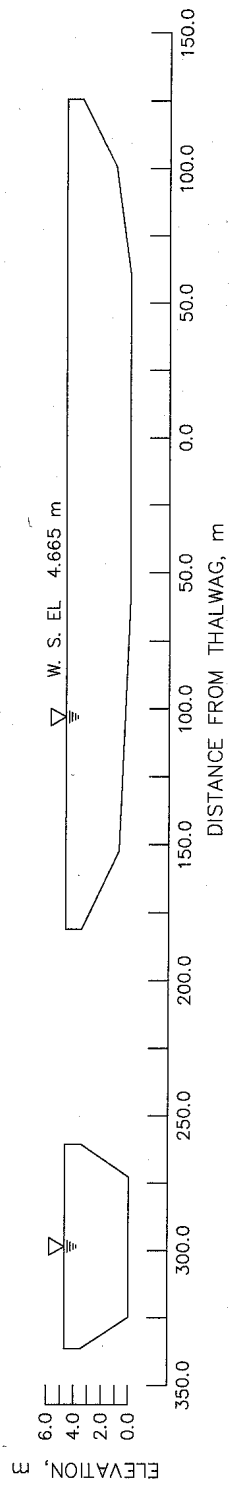


CLARK'S FERRY SITE
COMPUTED AND OBSERVED VELOCITIES
PROTOTYPE GAGE 1131

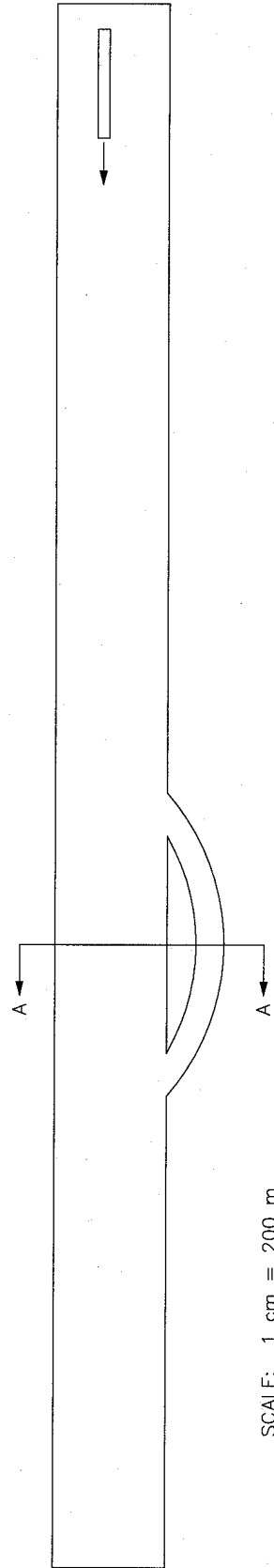


- NUMERICAL MODEL
- PHYSICAL MODEL – PROTOTYPE METER LOCATIONS (MAYNORD AND MARTIN 1998)
- PROTOTYPE (BHOWMIK, SOONG, AND XIA 1994)

RETURN CURRENT DISTRIBUTION DOWNBOUND TOW AT CLARK'S FERRY

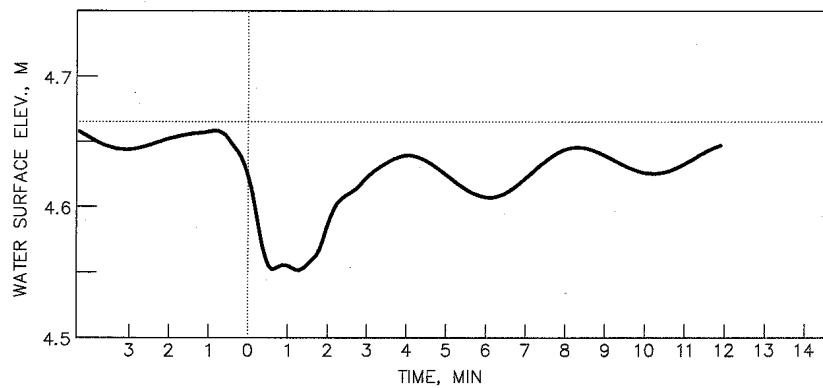


SECTION A-A

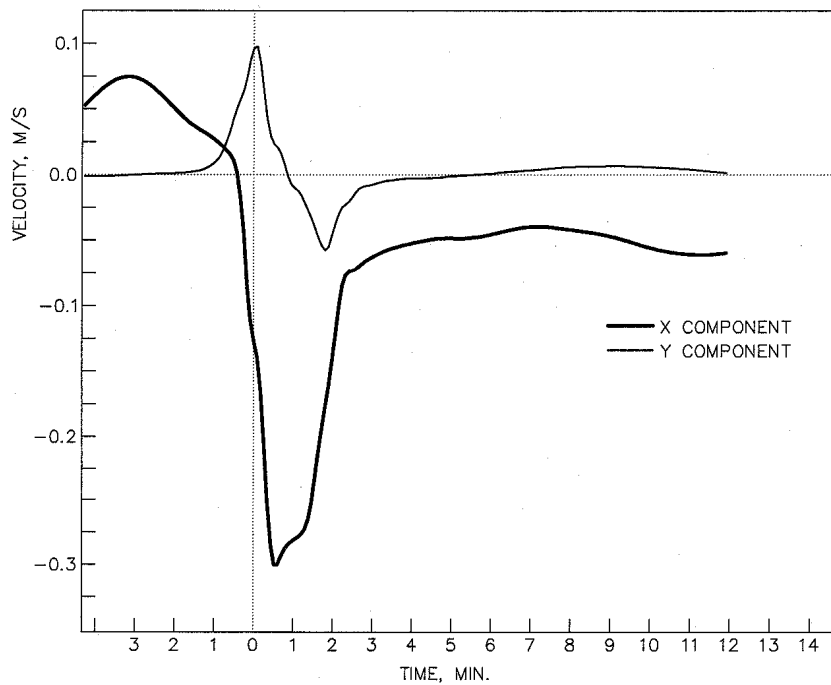


PLAN

SECONDARY CHANNELS
 $L/l=2.0$ $D/d=1.0$

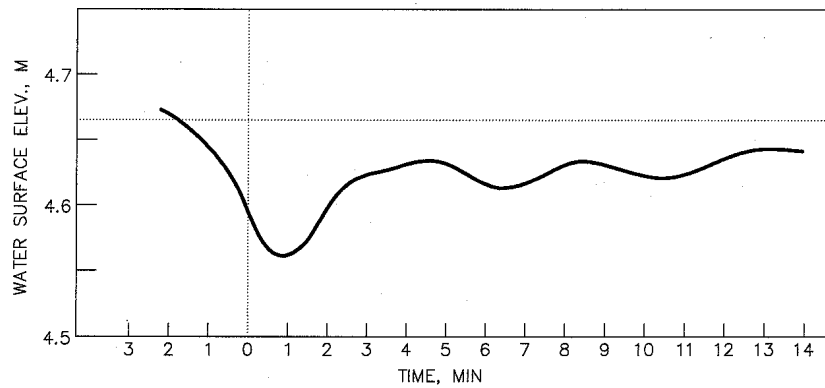


WATER SURFACE ELEVATION

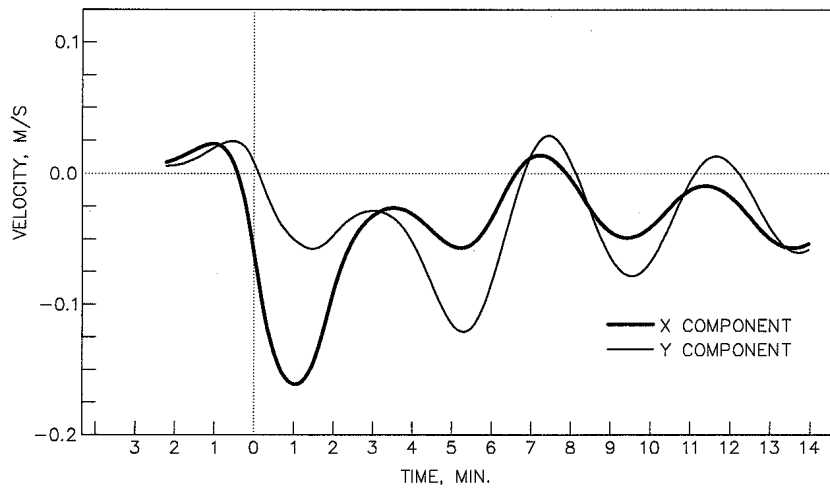


VELOCITY COMPONENTS

SECONDARY CHANNELS
 $L/l=2.0$ $D/d=1.0$
 MAIN CHANNEL

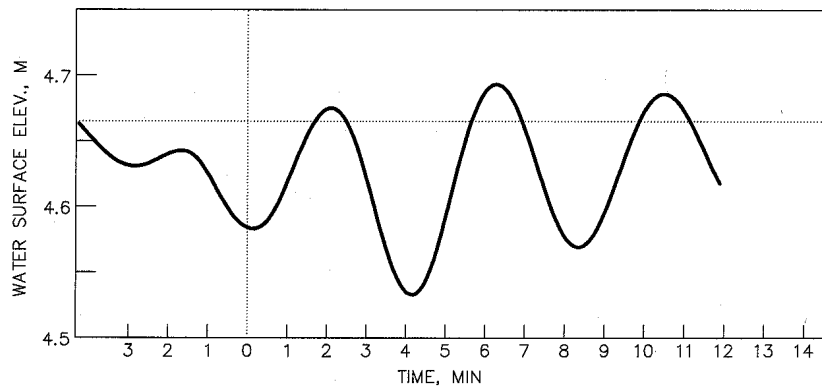


WATER SURFACE ELEVATION

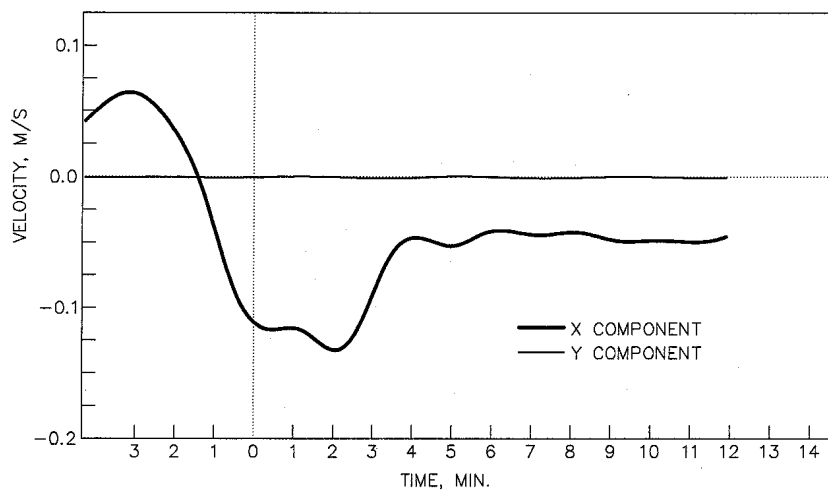


VELOCITY COMPONENTS

SECONDARY CHANNELS
 $L/l=2.0$ $D/d=1.0$
 INLET OF SECONDARY CHANNEL

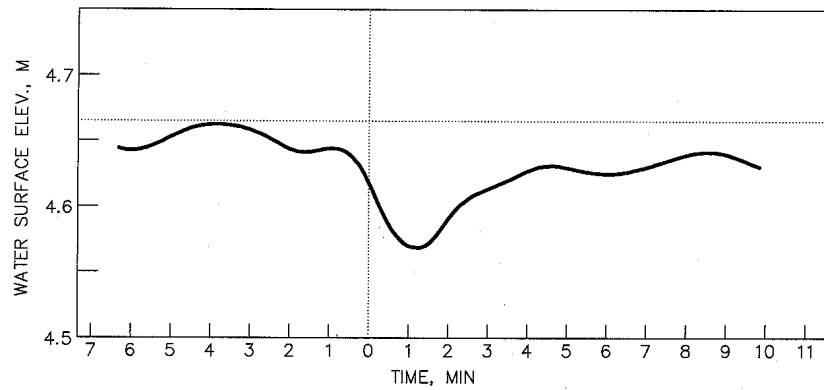


WATER SURFACE ELEVATION

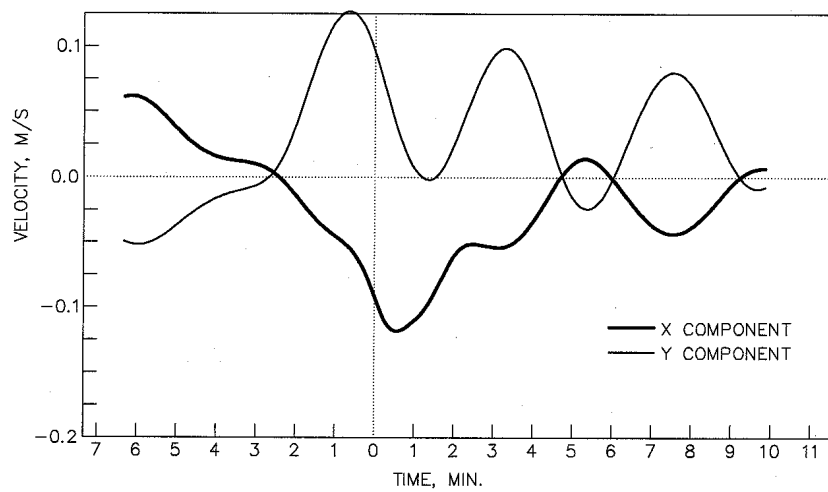


VELOCITY COMPONENTS

SECONDARY CHANNELS
 $L/l=2.0$ $D/d=1.0$
 MIDDLE OF SECONDARY CHANNEL

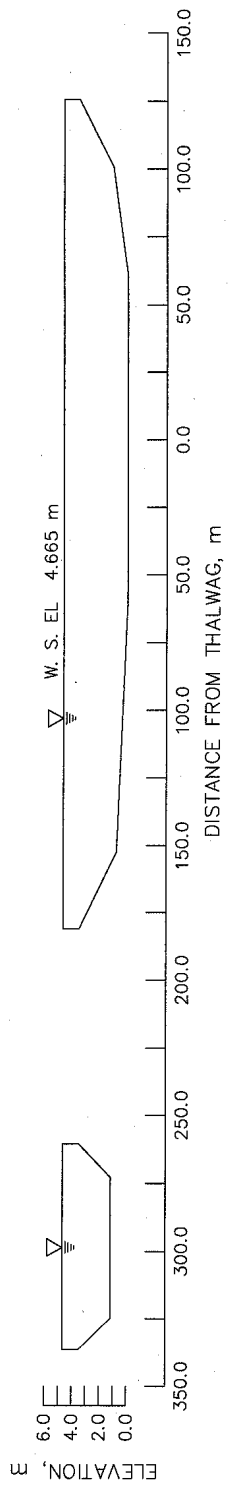


WATER SURFACE ELEVATION

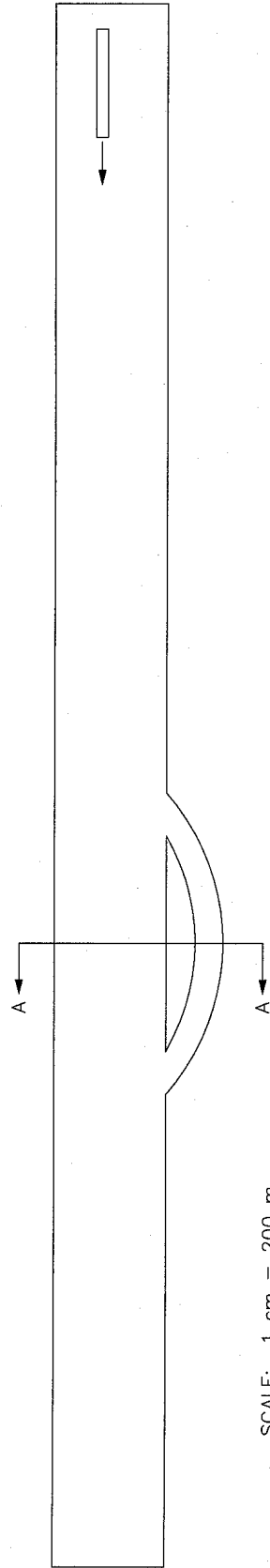


VELOCITY COMPONENTS

SECONDARY CHANNELS
 $L/l=2.0$ $D/d=1.0$
 OUTLET OF SECONDARY CHANNEL

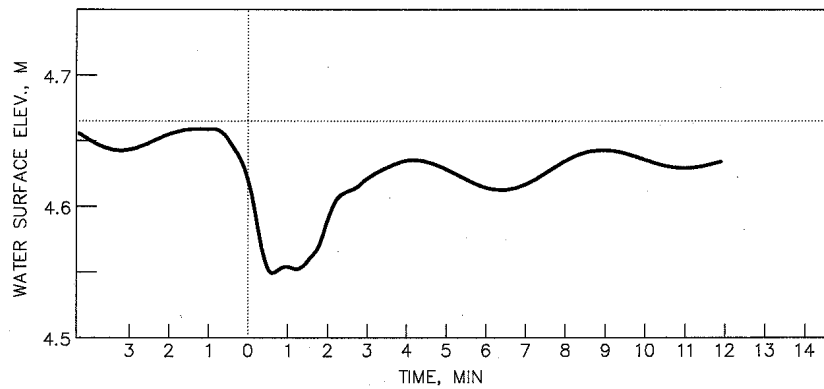


SECTION A-A

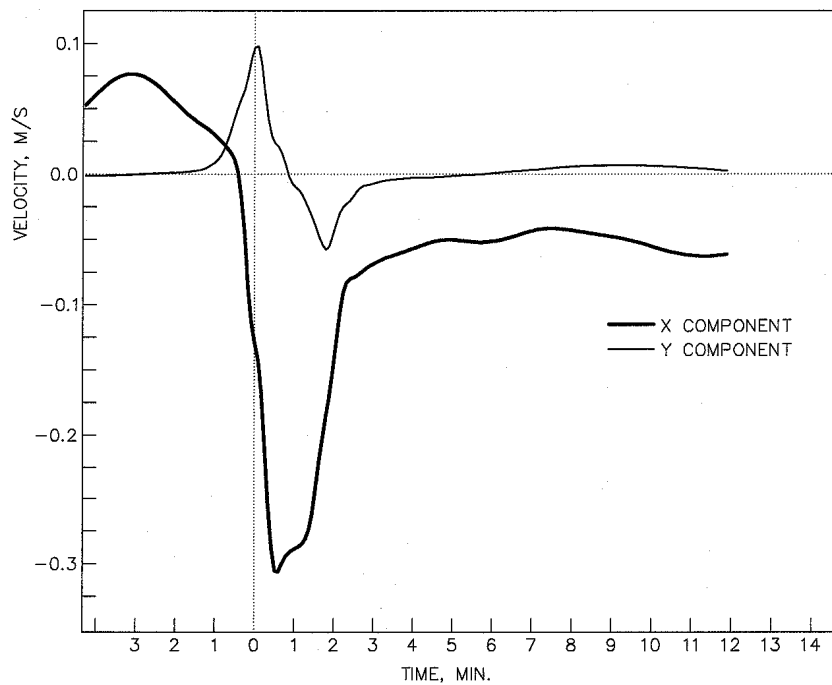


PLAN

SECONDARY CHANNELS
 $L/l=2.0$ $D/d=1.333$

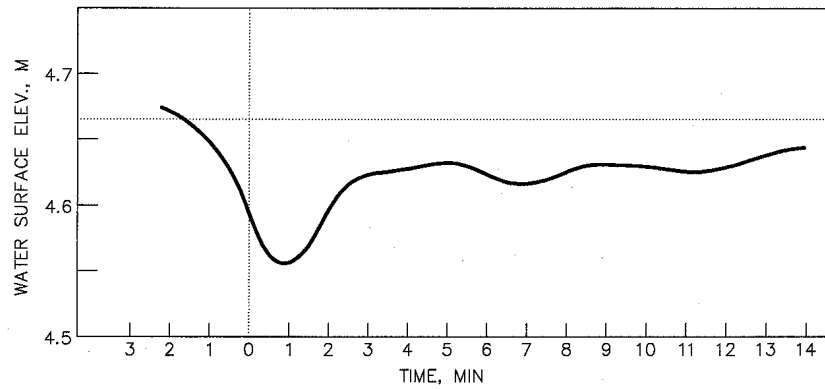


WATER SURFACE ELEVATION

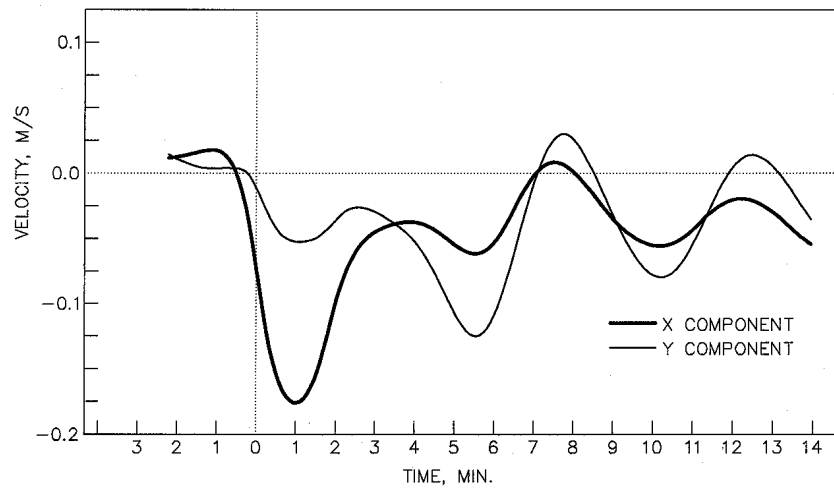


VELOCITY COMPONENTS

SECONDARY CHANNELS
 $L/l=2.0$ $D/d=1.33$
 MAIN CHANNEL

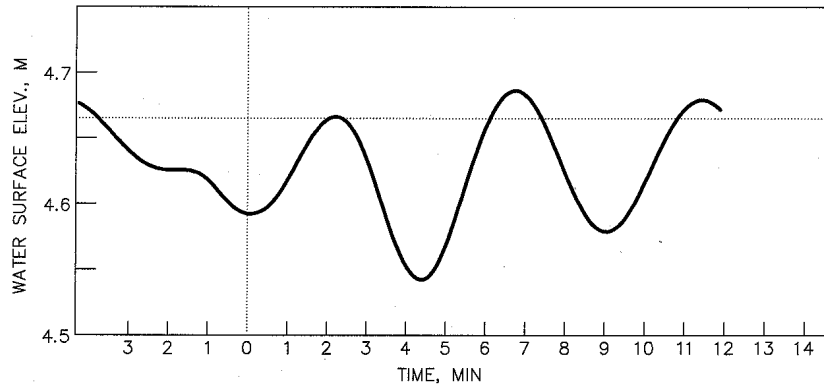


WATER SURFACE ELEVATION

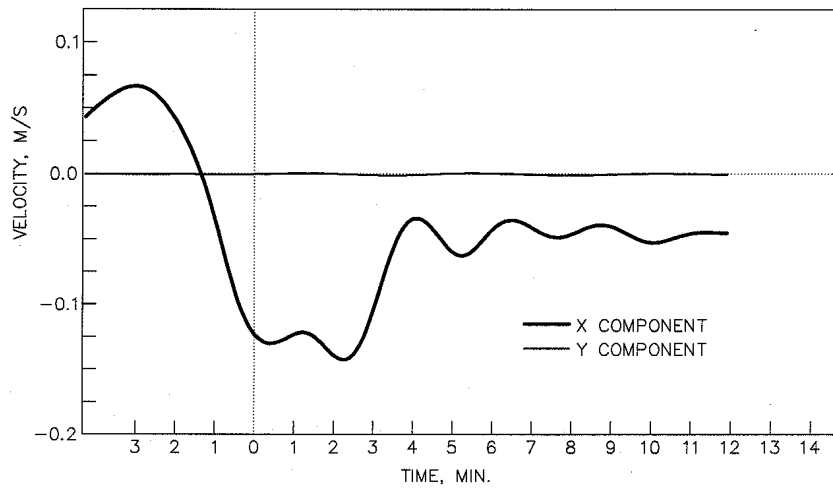


VELOCITY COMPONENTS

SECONDARY CHANNELS
 $L/l=2.0$ $D/d=1.33$
 INLET OF SECONDARY CHANNEL

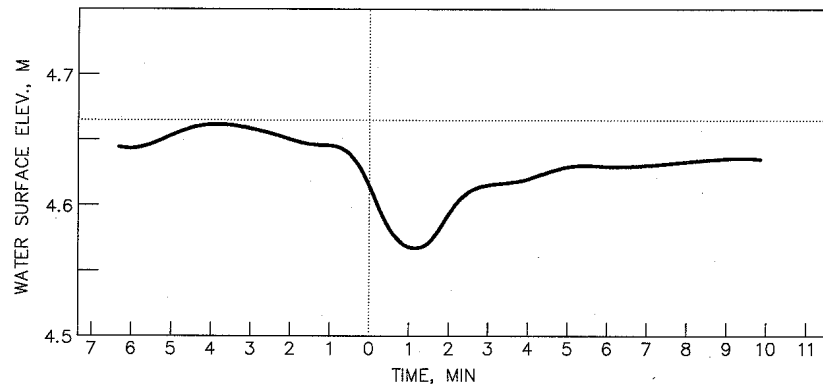


WATER SURFACE ELEVATION

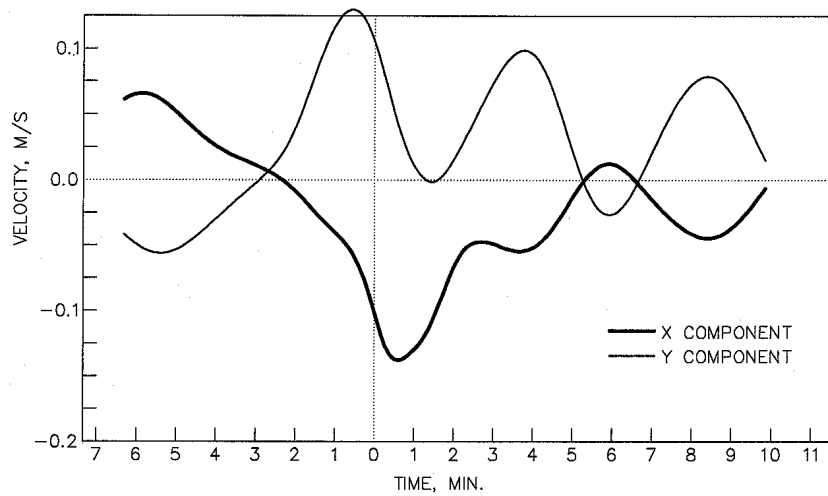


VELOCITY COMPONENTS

SECONDARY CHANNELS
 $L/l=2.0$ $D/d=1.33$
 MIDDLE OF SECONDARY CHANNEL

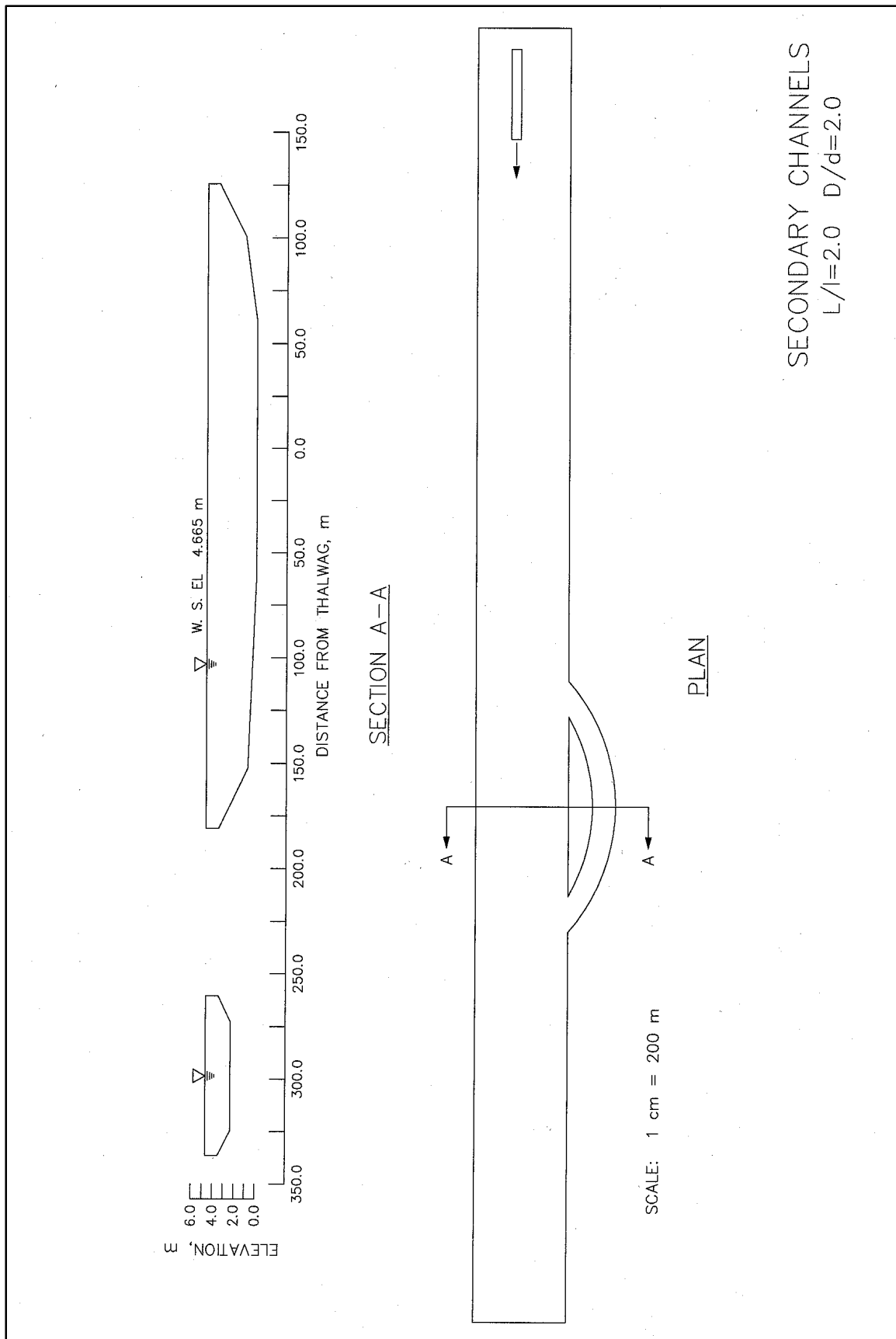


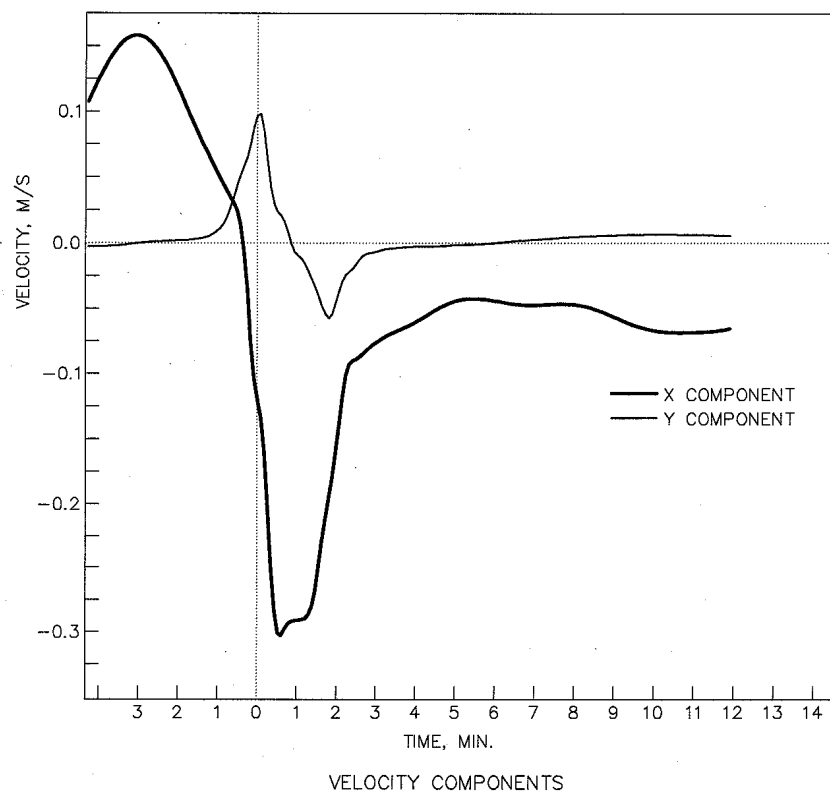
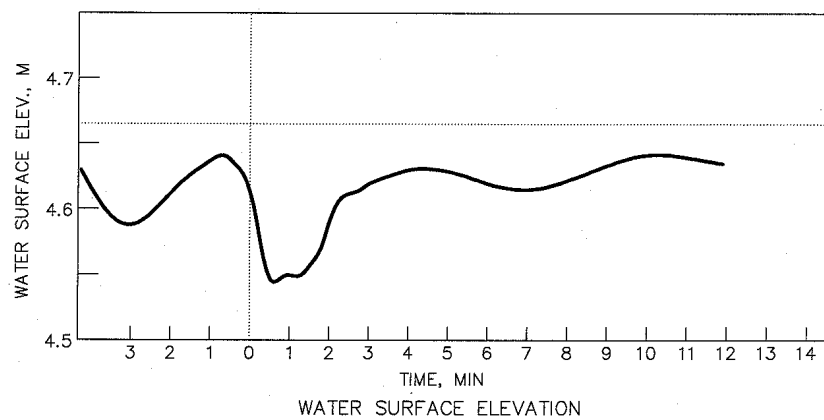
WATER SURFACE ELEVATION



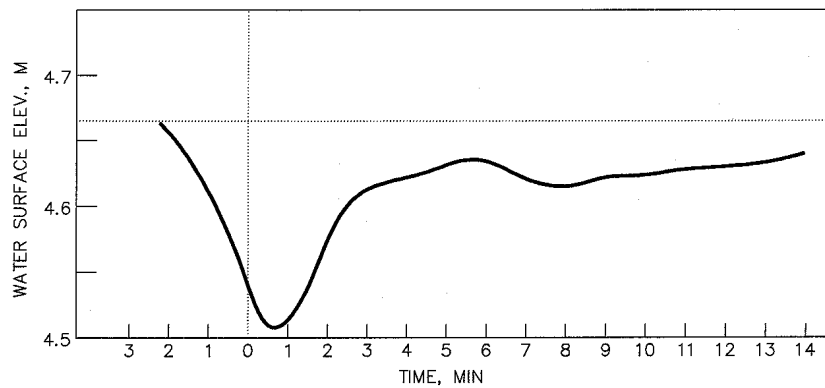
VELOCITY COMPONENTS

SECONDARY CHANNELS
 $L/l=2.0$ $D/d=1.33$
 OUTLET OF SECONDARY CHANNEL

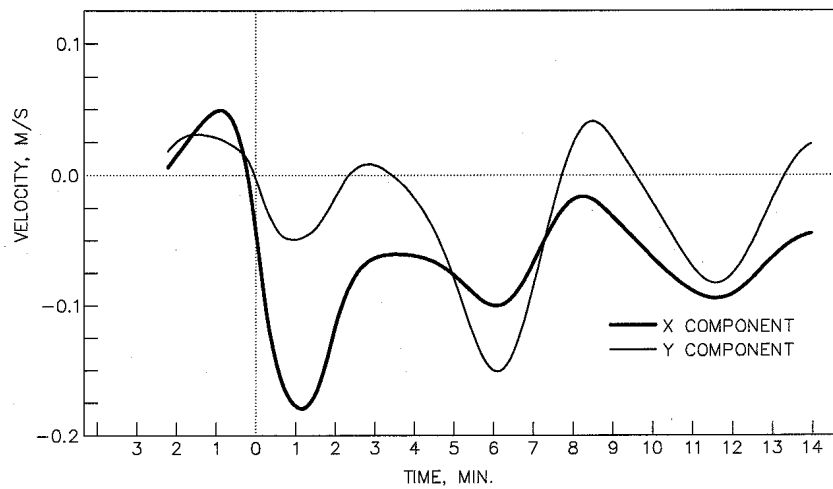




SECONDARY CHANNELS
 $L/l=2.0$ $D/d=2.0$
 MAIN CHANNEL

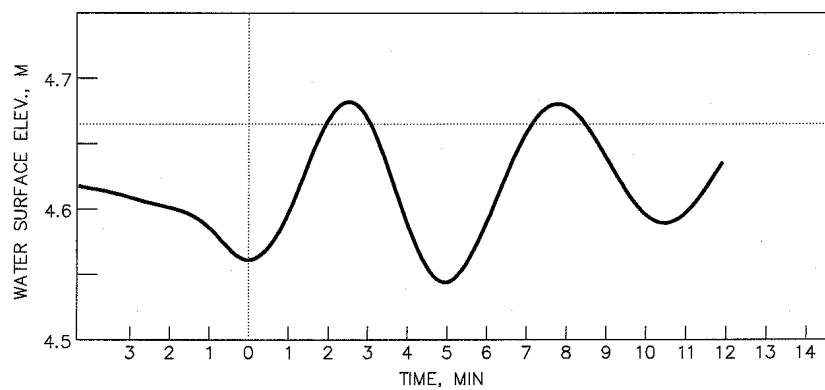


WATER SURFACE ELEVATION

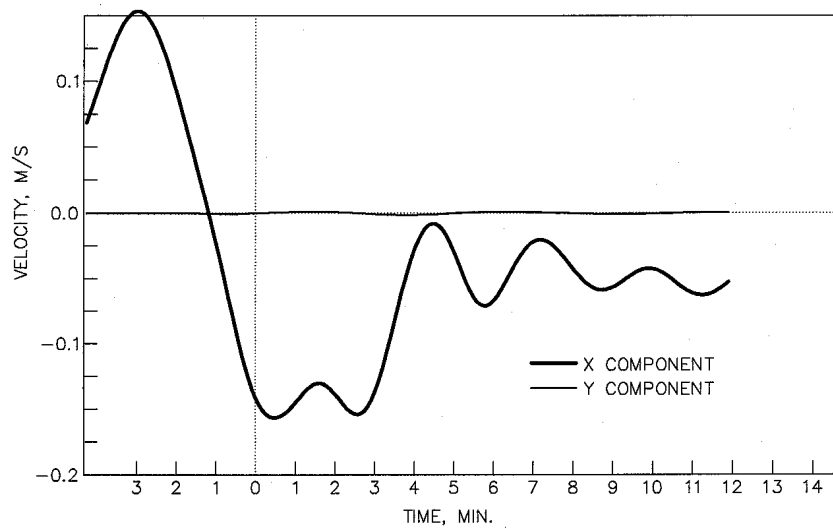


VELOCITY COMPONENTS

SECONDARY CHANNELS
 $L/l=2.0$ $D/d=2.0$
 INLET OF SECONDARY CHANNEL

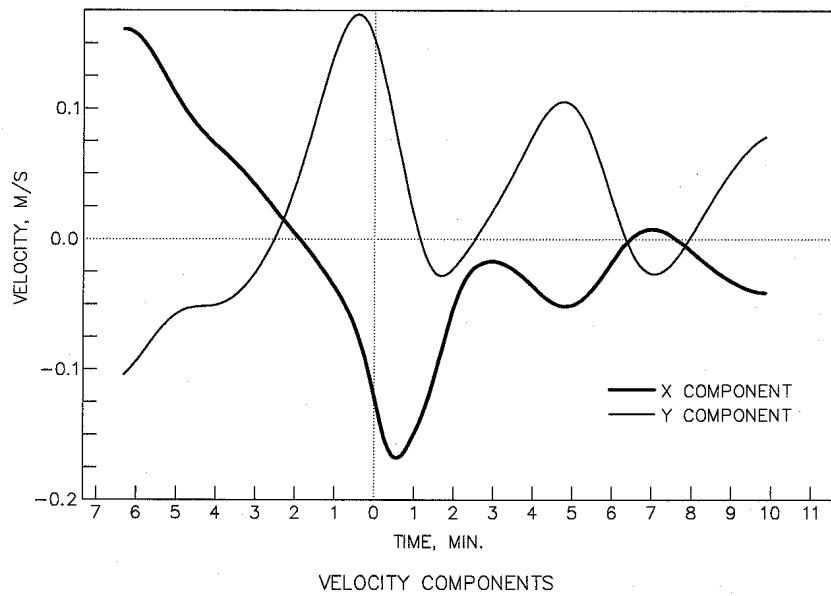
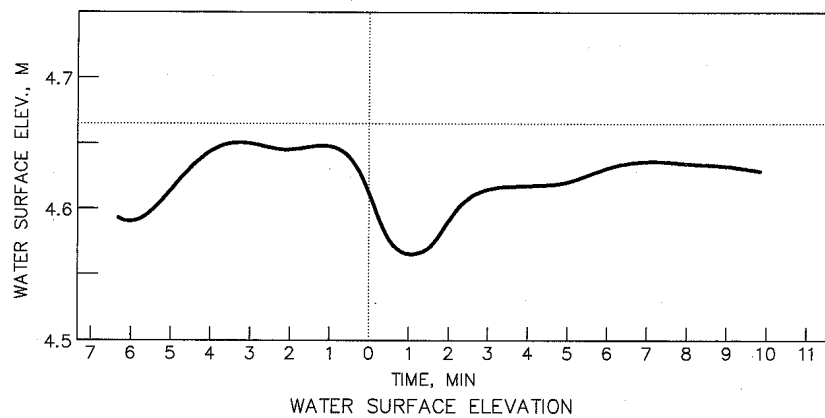


WATER SURFACE ELEVATION

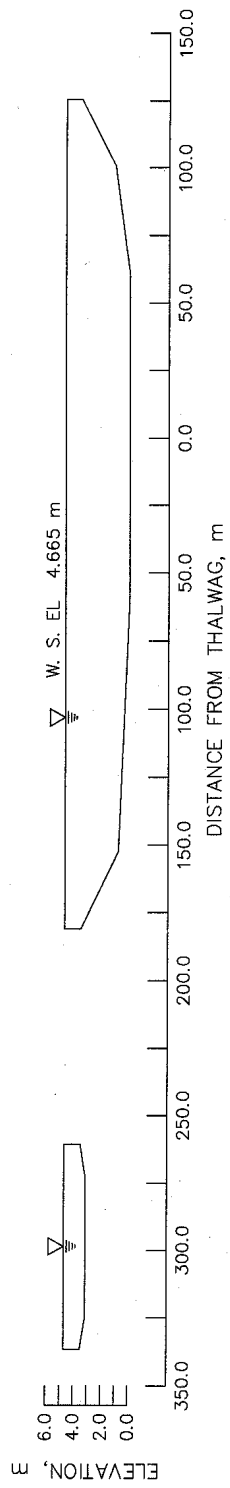


VELOCITY COMPONENTS

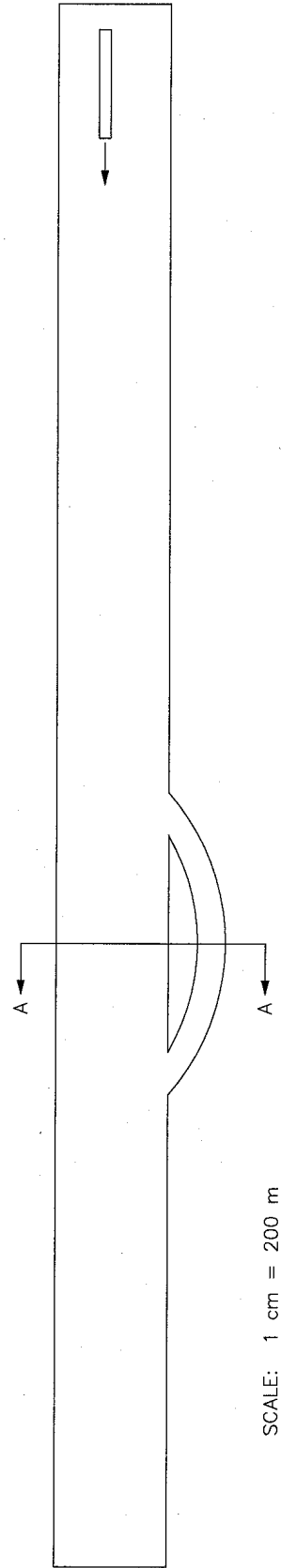
SECONDARY CHANNELS
 $L/l=2.0$ $D/d=2.0$
 MIDDLE OF SECONDARY CHANNEL



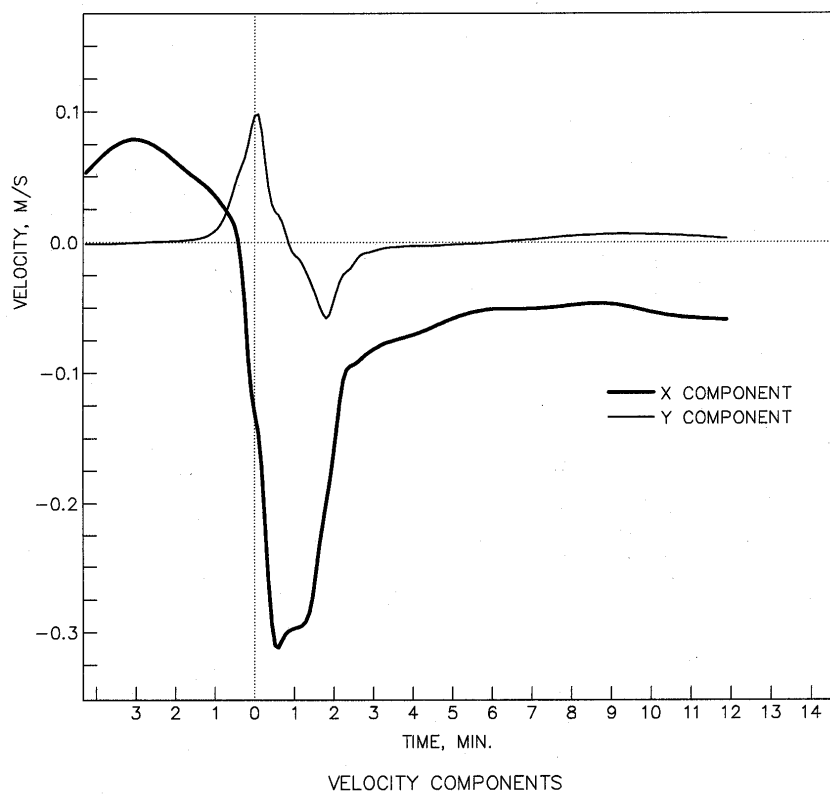
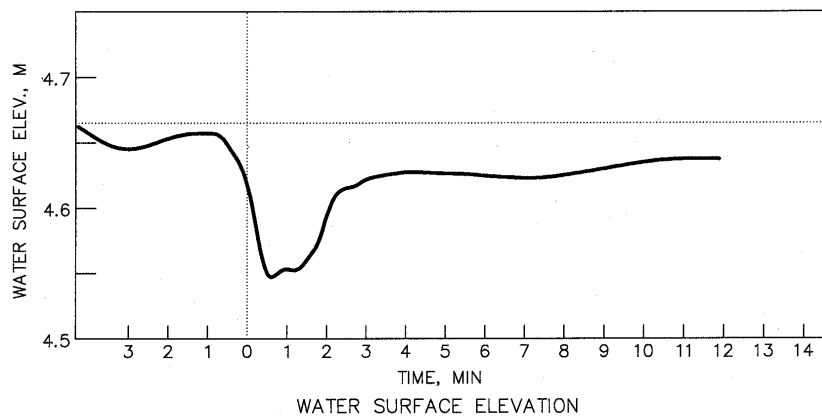
SECONDARY CHANNELS
 $L/l=2.0$ $D/d=2.0$
 OUTLET OF SECONDARY CHANNEL



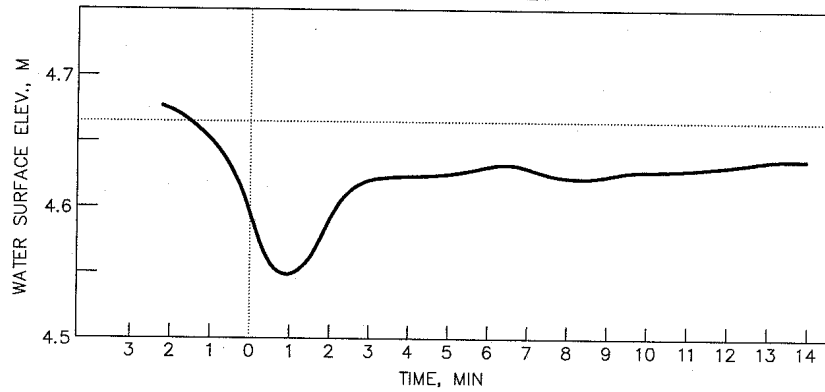
SECTION A-A



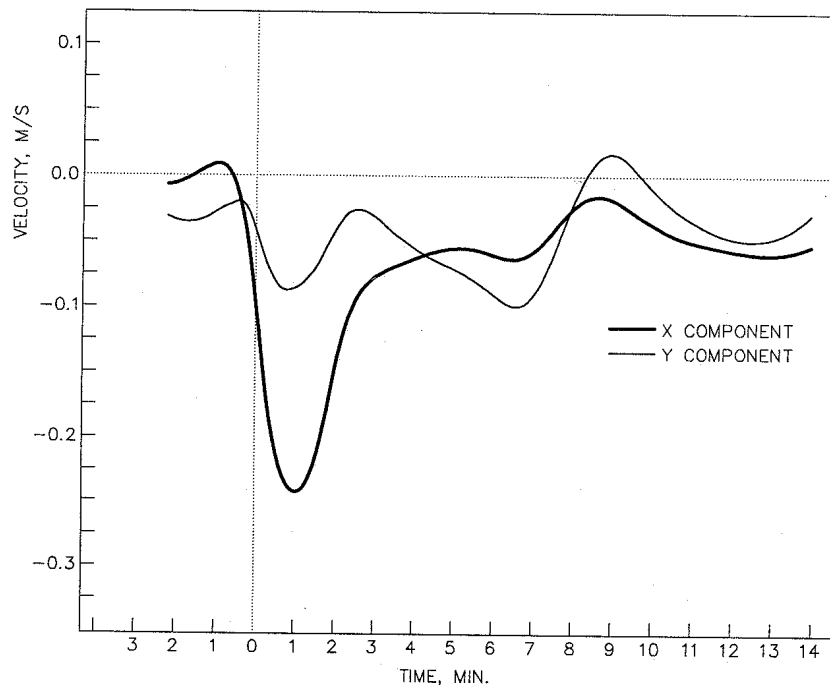
SECONDARY CHANNELS
 $L/l=2.0$ $D/d=3.0$



SECONDARY CHANNELS
 $L/l=2.0$ $D/d=3.0$
 MAIN CHANNEL

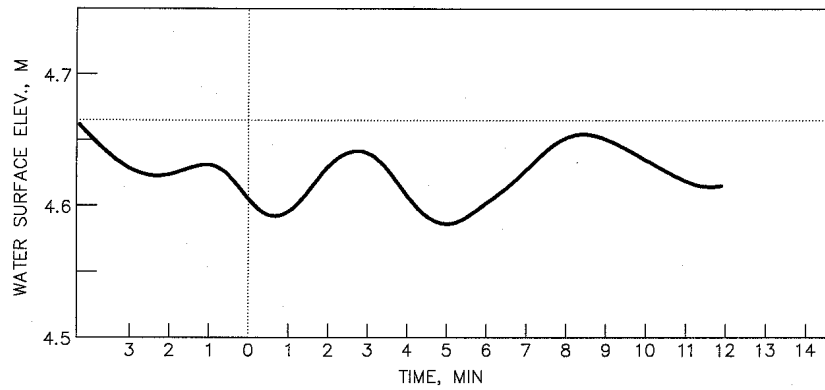


WATER SURFACE ELEVATION

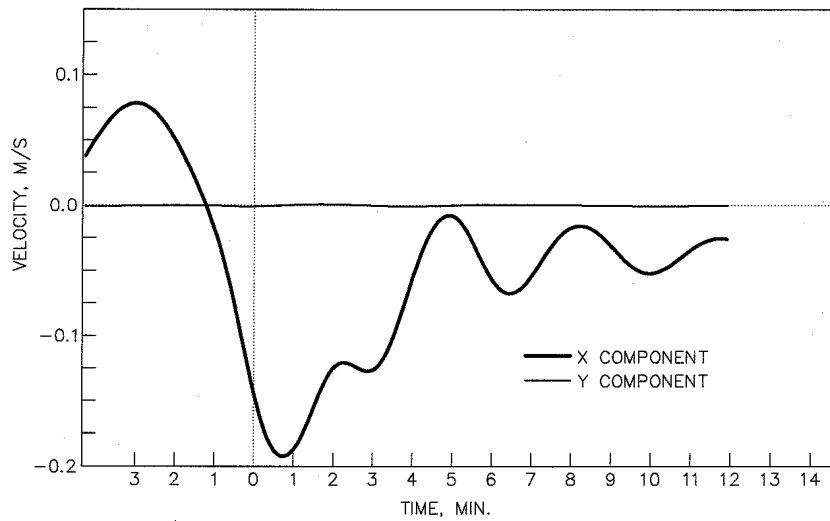


VELOCITY COMPONENTS

SECONDARY CHANNELS
 $L/l=2$ $D/d=3.0$
 INLET OF SECONDARY CHANNEL

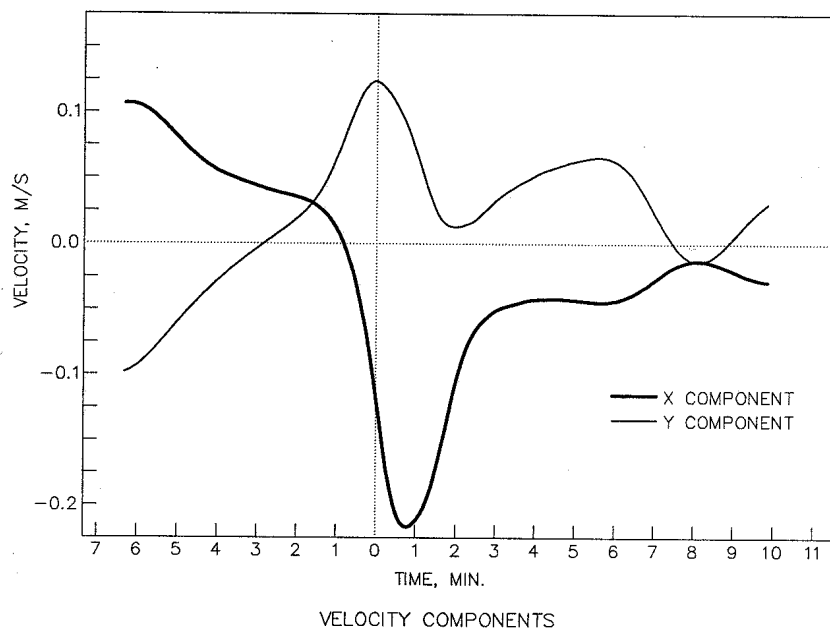
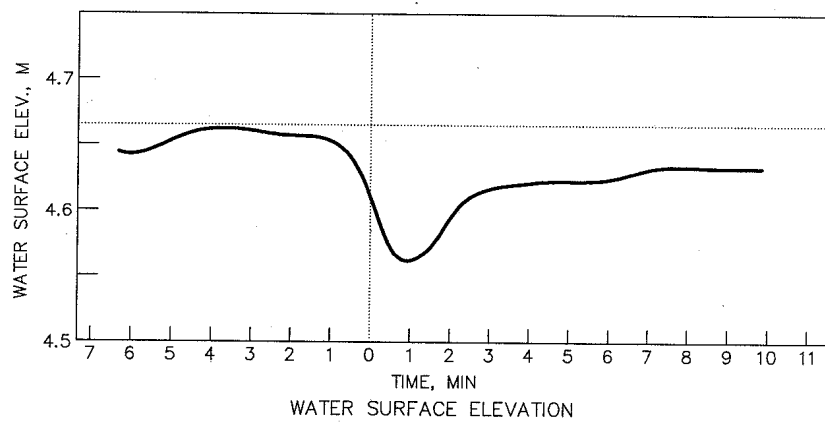


WATER SURFACE ELEVATION

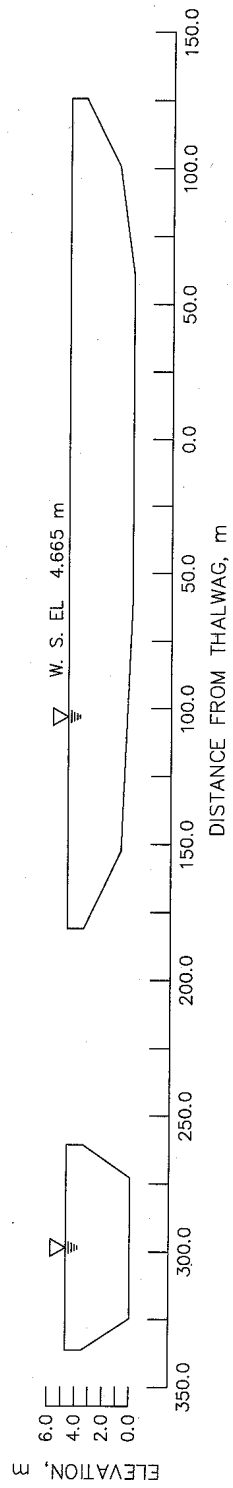


VELOCITY COMPONENTS

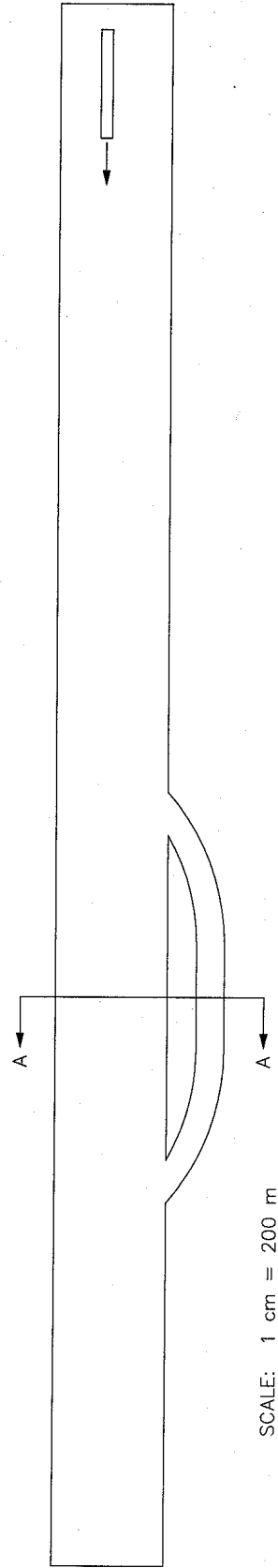
SECONDARY CHANNELS
 $L/l=2.0$ $D/d=3.0$
 MIDDLE OF SECONDARY CHANNEL



SECONDARY CHANNELS
 $L/l=2.0$ $D/d=3.0$
 OUTLET OF SECONDARY CHANNEL



SECTION A-A



SECONDARY CHANNELS
 $L/l=3.0$ $D/d=1.0$